2021-09

Simulation Modeling of Calgary's E-Scooter System

Mclean, Rachel

UNIVERSITY OF CALGARY

Simulation Modeling of Calgary's E-Scooter System

by

Rachel Mclean

A THESIS

SUBMITTED TO THE FACULTY OF GRADUATE STUDIES

IN PARTIAL FULFILLMENT OF THE REQUIREMENTS FOR THE

DEGREE OF MASTER OF SCIENCE

GRADUATE PROGRAM IN COMPUTER SCIENCE

CALGARY, ALBERTA

SEPTEMBER, 2021

Abstract

Shared micromobility is a rapidly growing transportation technology, with several companies establishing e-bike and e-scooter programs in cities across the globe. This thesis analyzes two years of empirical data on e-scooter usage from a shared mobility pilot program in the City of Calgary to create a synthetic workload model of e-scooter traffic. A synthetic workload generator is developed from this model and incorporated into a dedicated, custom-built simulation environment. This simulation is used to conduct experiments evaluating the impacts of different e-scooter management policies and infrastructure, such as fleet size, battery re-charging strategies, and urban parking infrastructure locations, on the efficacy of the shared e-scooter system. The results of these simulation experiments detail the impacts of these policies on satisfied user demand, costs of collecting depleted scooters to be recharged, and number of improperly parked scooters, and highlight the importance of proper site selection for parking areas and battery charging infrastructure.

Preface

This thesis is original, unpublished, independent work by the author Rachel Mclean.

Acknowledgements

First of all, I would like to offer my most sincere thanks to my supervisor, Dr. Carey Williamson, for his support as a teacher and mentor in my studies at the University of Calgary. He encouraged me to pursue exciting research opportunities as an undergraduate student and to pursue a graduate degree. His insightful questions and constructive feedback were a massive help in developing my research and polishing this thesis.

I would also like to thank Dr. Lina Kattan, my co-supervisor for her positivity and enthusiasm. Her wealth of experience in transportation systems continually pushed me to consider new lines of questioning.

I would like to thank the other members of my thesis committee, Dr. Faramarz Samavati and Dr. Merkebe Demissie for reviewing my thesis and providing their feedback, as well as for their questions and comments during my defense.

I would like to thank the NSERC-CREATE Integrated Infrastructure for Sustainable Cities (IISC - https://createiisc.com/) program for making this research possible, both by providing funding and by introducing a network of resources to draw on and like-minded researchers to reach out to. The program provided an excellent opportunity to broaden my horizons and explore new and innovative disruptions in urban development. In particular, I would like to thank Poornima Jayasinghe for her tireless work as Program Coordinator.

I would like to thank Spin, Lime, and Roll for answer some of my questions about e-scooters and shared e-scooter operations, as well as Andrew Sedor for meeting with me to discuss my research topics and sharing e-scooter data collected by the city of Calgary.

I would also like to thank NSERC for funding awarded via their CGS Master's scholarship, as well as Mitacs and LessThan3 for the funding and experience I gained through their Accelerate internship program.

Finally, I would like to express my deepest gratitude to my parents, Pamela Mclean and Dean Elhard, and to my sister, Anne Mclean, for their continued support and reassurance through all the ups and downs of my graduate program.

Table of Contents

List of Tables

List of Figures

List of Symbols, Abbreviations, and Nomenclature

CO2	Carbon Dioxide
e-scooter	Standing electric scooter
EV	Electric vehicle
ITT	Inter-trip time
kJ	Kilojoules
kph	Kilometres per hour
KS	Kolmogorov-Smirnov
li-ion	Lithium Ion
mps	Metres per second
QQ Plot	Quantile-Quantile Plot
SMMS	Shared Micromobility Service
SNG zone	Share-And-Go parking zone
SOC	State of Charge
Wh	Watt hours

1 Introduction

1.1 Motivation

Since 2017 [16], more and more cities around the world have become host to a growing population of shared standing electric scooters (e-scooters). These are the latest technological development within the increasingly popular domain of shared mobility transportation modes, which have historically ranged from car-sharing services like Car2Go (now ShareNow[1]) or ZipCar[2], to ride-sharing services like Lyft[3] or Uber[4], to docked or dockless bike-sharing services like those offered by Lime[5].

In only a few years since their introduction, scooter-sharing programs have seen a much greater and more rapid adoption than either car-sharing or bike-sharing programs [16], [34]. In 2018, only a year after shared e-scooter services became available in the United States, Bird had already expanded its operation to over 100 cities around the world [62], and by 2021 that number had increased to more than 250. Lime – which also launched in 2017 – reported 26 million e-scooter trips using their service by December of 2018 [28]. A report of shared micromobility in the US released by NACTO (National Association of City Transit Officials) the same year showed that the number of shared scooter trips across the United States was already comparable to the number of shared bicycle trips [34] and their subsequent report in 2019 showed that e-scooter trips had far outstripped shared bicycle trips by a factor of two to one [35]. By 2030, micromobility

[1] https://www.share-now.com/
[2] https://www.zipcar.com/
[3] https://www.lyft.com/
[4] https://www.uber.com
[5] https://www.li.me

programs including bike- and scooter-sharing could achieve a market potential of $200-300 billion US [20].

In 2018, the City of Calgary announced a new, two-year shared mobility pilot program that introduced dockless e-bikes and e-scooters throughout the city. Over the two years, the city partnered with Lime, Bird[6], and Roll[7] to supply shared mobility vehicles and record trip statistics for characterizing traffic patterns. In 2019, the city conducted a survey whereby Calgarians, e-scooter users and non-users alike, were invited to provide their input on the pilot program and identify particular benefits or areas of concern [56]. The results of the survey suggested that there were some concerns about the safety of sharing pedestrian pathways with e-scooter users and about the inconvenience of abandoned or improperly parked scooters. Nonetheless, most Calgarians believed there was substantive benefit to having an additional mode of transportation available. Despite the disruption of the COVID-19 pandemic and its associated public health restrictions, the pilot program continued successfully through 2020, and in the spring of 2021, the City opted to continue private sector shared micromobility services (SMMS) in partnership with Bird and Neuron[8][58].

Given the recent but rapid emergence of shared e-scooters as innovative disruption within the field of transportation, the currently available research on this particular mode of shared micromobility remains limited, but there can be no question about the value of such research. In a world that is becoming increasingly urbanized, shared mobility services may reduce the reliance on private motor vehicle ownership, consequently reducing traffic congestion and potentially the demand for associated motor vehicle infrastructure such as parkades, on-street parking, and wide,

[6] https://www.bird.co/
[7] https://www.rollscooters.com/
[8] https://www.rideneuron.com/

multilane roads [16]. Deemphasizing the importance of private vehicles may also expand transportation access for low-income individuals by eliminating the upfront cost of a personal motor vehicle, which can act as a barrier to entry [48]. Shared bikes and scooters in particular may have direct environmental benefits by offering a zero-emission alternative to motor vehicles. These vehicles are more strictly range-limited than motor vehicles, making them well-suited to short trips including first-and-last-mile transportation that can help to facilitate public transportation. But for all their promise, these new technologies bring new challenges for operators and policy makers who must balance concerns about curb space management and the safety of e-scooter users and non-users with the growing demand for varied transportation options. Addressing these challenges requires careful analysis and the development of flexible tools to guide future policy decisions.

The hypothesis of this thesis is that simulation is a promising approach to investigate the shared micromobility problem domain. In general, simulation is an effective tool for scenario analysis and policy recommendations, particularly in large systems where implementing changes can be expensive and potentially have negative impacts on the users of those systems. Discrete-event simulation in particular can allow for efficient scalability of the simulation model and manageable runtimes, while accommodating data gaps surrounding the interacting behaviours of agents within the system. Discrete-event simulation modeling is the primary approach adopted in this thesis.

1.2 Research Objectives

The primary research questions for this thesis are as follows:

- What are the key characteristics of e-scooter traffic in downtown Calgary?

- What are the primary challenges of implementing an effective shared e-scooter program in terms of costs to e-scooter operators, users, and non-users?
- How can those challenges be addressed or mitigated through changes to e-scooter management policies or infrastructure dedicated to facilitating shared e-scooter programs?

To answer these questions, a workload characterization is conducted using two years of empirical e-scooter data in downtown Calgary. Furthermore, a discrete-event simulation model is constructed from that characterization to represent the e-scooter system in downtown Calgary with a particular focus on e-scooter supply, fleet management strategies, and infrastructure needs for the e-scooter system.

1.3 Contribution of the Thesis

Although the amount of research into shared e-scooter programs is quickly growing [1], much of this research is focused on establishing definitions within the field [49], [50], [51], identifying policy challenges or potential benefits [4], [21], [23], [30], [37], [59], and interpreting public attitudes towards these programs. Some studies have conducted analyses of rider behaviour and traffic patterns [10], [24], [31], [32], [43], but only three have attempted to use discrete-event simulation to optimize the operation of shared e-scooters. Two of these were focused specifically on the challenge of relocation to maintain an optimal geographical distribution of e-scooters [19], [60]. The third, which examined the impact of e-scooter fleet size, variable low-charge threshold, and collection and redistribution strategies on operator costs and ability to satisfy user demand, was conducted using data from Louisville and Minneapolis in the United States [13].

The research contained in this thesis attempts to address policy questions regarding appropriate fleet size, dedicated e-scooter parking, and battery charging strategies, using the City of Calgary's shared mobility pilot program as a case study. This work presents a detailed analysis of the publicly available e-scooter trip data from 2019 and 2020 to identify specific trends as well as distributions of individual trip characteristics, and describes the development of a customized discrete-event simulation model and dedicated simulation environment for examining the impact of policy changes to the e-scooter system.

1.4 Organization of the Thesis

The structure of this thesis is as follows. Chapter 1 introduces the problem and gives a brief overview of the rest of the thesis. Chapter 2 provides a review of the relevant literature, including research related to shared mobility, E-scooter and electric vehicle (EV) technology, and discrete-event simulation. Chapter 3 examines the available data and develops a workload characterization with consideration for trip volume and characteristics. Chapter 4 describes the simulation model, including the type of simulation used, the simulation environment, the synthetic workload generation, and the simulation validation. Chapter 5 is a discussion of the experiments conducted and their results. Chapter 6 concludes the thesis and provides suggested directions for future research.

2 Background and Related Work

This chapter provides a brief overview of the literature regarding shared micromobility and simulation modelling. Section 2.1 provides a summary of shared mobility and micromobility technologies and their role within the evolving transportation landscape. Section 2.2 describes the benefits and applications of workload characterization from empirical data and provides a review of workload characterization studies relating to shared mobility. Section 2.3 provides a review of simulation studies relating to shared mobility and discusses the necessary tools for developing a shared micromobility simulation model. Section 2.4 summarizes the chapter.

2.1 Shared Micromobility

2.1.1 Definitions

Shared mobility refers to the broad umbrella of transportation services existing within the sharing economy, which includes peer-to-peer or centralized vehicle-sharing programs (i.e., Lime, Car2Go, ZipCar), ride-sharing and ride-sourcing services (i.e., Uber, Lyft), and alternative transit services like shuttles, buses, or rail transit [49]. This sharing structure allows users to have access to specific modes of transportation only as needed and for short periods of time, reducing the proportion of time when a vehicle sits idle or empty and reducing the cost to the individual of regular vehicle maintenance.

Shared mobility is a concept that has existed within urban environments for generations, through car rentals, taxi services, and public transportation [54]. Small scale bike-sharing programs were in operation as early as 1965 in Amsterdam [1]. Throughout the 1990s, car-sharing was already being touted as a viable and innovative alternative to private car ownership [52]. However, shared mobility services saw a distinct surge in the wake of the recession of 2007-2009, along with

a shift towards integrating smart phone technology. Through the years that followed, several shared mobility services with integrated smart-phone apps, such as ZipCar, Uber, and Lyft, rapidly emerged as popular transportation options [51].

In more recent years, the landscape of shared mobility services has begun to shift again with the emergence of limited-speed, single-occupant shared vehicles, like human-powered or electric bikes, moped-style scooters, and standing e-scooters such as those shown in Figure 2.1.

Figure 2.1: A row of Lime brand shared e-scooters in Berlin, Germany (Photo by Vince Jacob on Unsplash)

These shared mobility modes fall under the narrower definition of *shared micromobility* [50] and fulfill different niche requirements than car-sharing or ride-sharing services because of their limited capacity and reduced range. The wide use of GPS tracking technology, geo-fencing, and integrated smart-phone applications also allows for these shared mobility fleets to be managed

without the necessity of centralized kiosks or storage areas, allowing for much greater flexibility in how, when, and where the vehicles are used.

2.1.2 Potential Benefits and Challenges

Increasing urbanization, particularly in conjunction with broad urban sprawl, has created a high reliance on private vehicle ownership, which in turn has given rise to a series of social, economic, and environmental concerns. One of the strongest driving factors behind the adoption of shared mobility and shared micromobility in particular is its potential to alleviate some of these concerns.

Growing traffic volumes have resulted in congested streets and reduced traffic flow, with the average driving speed in many cities falling below 20 kph [18]. Approximately 80-90% of automobile travel is made up of short car trips transporting a single person. Because micromobility vehicles have a lower range than motor vehicles, and because they can only accommodate a single occupant, e-scooters could be used as an effective replacement for many of these trips, and the subsequent decrease in cars on the road would decrease congestion [16]. Moreover, a single user riding a powered micromobility vehicle takes up a much smaller footprint on the road or sidewalk, suggesting that with changes in dedicated infrastructure, a much higher number of e-scooter travellers could be accommodated before encountering similar congestion issues. A study of e-scooter users in Paris suggested that although most of the considered shared e-scooter trips were substituted for walking or public transportation trips, 16% replaced private car trips [12].

Shared micromobility services (SMMSs), particularly those using dockless, free-floating fleets of micromobility vehicles, are also very well suited for first-and-last-mile transportation, effectively bridging the gaps in existing public transportation infrastructure [16], [29], [49]. As a result, shared-micromobility services can reduce travel times[1], thus making public transportation

both a more appealing option for many people who would otherwise default to the use of a private motor vehicle, and a more viable substitute for those without reliable access to a private motor vehicle.

Both through direct substitution of private motor vehicle travel and supplementation of public transportation options, SMMS have the potential to substantially reduce CO2 emissions from urban travel. A shared e-scooter pilot program that ran in Portland in 2018 estimated that the number of trips substituting e-scooters for automobiles had resulted in a reduction of approximately 122 metric tonnes of CO2 [39]. However, some studies have suggested that this benefit is strongly mitigated, or perhaps even eclipsed, by the environmental costs of production and the emissions from motor vehicles used to collect and redistribute SMMS fleet vehicles, emphasizing the importance of longer life cycles for powered micromobility vehicles and efficient management strategies for SMMS operators [21].

The concerns about the true environmental impact of SMMS highlight a broader point, that without rigorous and carefully examined regulation, these services will likely fall short of their promised potential and introduce a host of new issues associated with the services themselves. Municipal governing bodies are now faced with the questions of how – or whether – to facilitate the development of SMMS in their cities while working to address the new challenges that they present. These questions include where and how e-scooters may be ridden and parked, such as restrictions to roads, sidewalks, or bike lanes, and the maximum speed limit for e-scooters; the minimum safety requirements for using e-scooters, such as mandated helmet usage, minimum age, and maximum occupancy limits; and how to appropriately share public spaces with pedestrians and other vehicles [30], [37].

Both the mid-pilot and final report on Calgary's shared mobility program listed safety as one of the primary concerns related to the program [46], [47]. In fact, the safety of both users and non-users is a common theme in studies of attitudes and policies regarding e-scooter usage [30][36]. A study of e-scooter injuries resulting in calls to EMS was conducted in Copenhagen and found that most injuries reported were a result of falling off the scooter rather than collisions with an object, person, or vehicle [8]. The same study found that very few patients were wearing a helmet at the time of the accident, and that alcohol or drug intoxication was present in approximately one-third of e-scooter patients.

Micromobility modes like bikes and scooters represent a hybridization of transportation, somewhere between a road vehicle and pedestrian, which may allow users to switch between modes when convenient [61]. Although most e-scooter riders prefer to use bikeways, they are likely to default to pedestrian pathways when bikeways are limited and road traffic is travelling at high speeds [39]. Thus, another frequent concern, particularly among non-users, is the infringement of SMMS vehicles and traffic on pedestrian areas [59]. Shaheen & Cohen [50] refer to this issue as curb space management, and list a number of policies for reducing e-scooter clutter on city curbs, including fleet size caps that limit the number of SMMS vehicles, designated parking areas for SMMS vehicles, and fees or fines for parking SMMS vehicles in public spaces. However, such policies must be carefully examined since efforts to restrict the placement of SMMS vehicles may not appropriately match the shift towards *dockless* shared mobility modes that has driven much of the demand for e-scooters in particular [36].

2.2 Data Analysis and Workload Characterization

Understanding traffic flows and patterns in user behaviour is a crucial component of evaluating and improving the performance of a system. Several studies have been conducted in

recent years to characterize the usage patterns of shared mobility users. A study of Uber vehicle movements and ride requests in San Francisco and Manhattan identified key differences in the application of surge pricing between the two cities and recommended strategies for Uber users to avoid surge pricing when requesting a ride [11]. Another study, conducted in Chengdu, China, analyzed the use of 'ride-splitting' versus single-user ride-sourcing programs and found that although the current adoption rate of ride-splitting is small, it has the potential to reduce travel times by 22% [27]. Most recently, a study of three different car-sharing services in Vancouver compared usage patterns between services and public transportation modes with the goal of informing urban planning [2].

As e-scooters have emerged as a popular alternative mode of shared mobility, more and more studies have attempted to characterize the population of e-scooter users and their usage patterns. A study of factors influencing mode-choice between docked or dockless e-bikes and dockless e-scooters in Zurich suggested that bikes are still preferred to scooters for longer or uphill trips, but that adverse weather was a stronger deterrent against use of a shared bike than use of a shared scooter [43]. A similar study of shared bike usage conducted in Beijing four years earlier also noted the negative impact of poor weather and air quality on the bike usage, particularly over more sheltered modes of transportation [9].

In 2020, multiple studies were published that discussed the spatial associations [10] and trip characteristics [24] of shared e-scooter usage in Austin, TX between 2018 and 2019. These found that the density of e-scooter trips tended to be higher in areas with high population density, lower household income, and higher levels of education, such as in areas surrounding university campuses or downtown areas. Surveys of private and shared e-scooter users were conducted in France to characterize their demographic distribution and reasons for using the scooters [12], [61].

Another 2020 study used text-mining from social media and machine learning to gauge public opinion about shared-micromobility programs, noting that public interest in shared e-scooters was on the rise [41].

2.3 Simulating Transportation Systems

Although the field of SMMS research relating to shared e-scooters is still emerging, shared mobility more generally has existed in some form for decades. As such, there is a wealth of simulation research on other modes of shared mobility services that can inform research on e-scooters and shared e-scooter programs.

In 2013, Clemente et al. identified the key determinants of shared mobility performance as: (1) optimal fleet size, (2) location of parking areas, (3) pricing policies, and (4) flexibility. They then used discrete-event simulation to assess the performance of a two-station car-sharing service model [14]. A 2001 paper outlined a set of performance metrics for managing the geographic distribution of vehicles in a station-based shared vehicle service [7]. In the years since, several papers have addressed the issue of vehicle distribution and relocation in different shared mobility and micromobility modes using dynamic routing of collection vehicles in conjunction with cost incentives for the user [38], defining geo-fenced areas of operation using k-clubs [42], and utilizing autonomous shared vehicles [44]. In 2017, a study using agent-based simulation assessed the efficacy of an autonomous shared mobility network in Melbourne and determined that the incorporation of autonomous vehicle technology reduced the total number of vehicles needed to satisfy demand within the service area [15].

Most recently, some studies have examined strategies specifically for e-scooter battery charging and fleet management using simulation models. In 2018, a small pilot study was

conducted at a university campus in Taiwan that used battery-swapping stations and real-time location information about e-scooter use to extend the effective range of the e-scooters [55]. In 2020, a larger simulation study of battery-swapping stations at high-traffic tourist locations in Taiwan outlined an efficient algorithm for placing stations and deploying batteries [63]. Other studies have focused on the established problem of vehicle distribution as it applies to fleets of shared e-scooters, using crowd-sourced repositioning [19] or using responsive algorithms to guide operators in relocating vehicles [60]. Lastly, a 2020 study leveraged public e-scooter data from Louisville and Minneapolis to create a simulation model and synthetic workload generator. These were then used to assess the impact of fleet size, low-battery charging threshold, and battery charging policy on the ability of the e-scooter fleet to satisfy user demand [13].

2.3.1 Simulation Software

Simulation modeling is a general-purpose technique from the field of performance evaluation that can be used to assess the performance characteristics of a system. This type of modeling involves identifying the key actors within the system to be modelled and the primary events that change the state of the system. The model may then be used to track how the state of the system changes over time and in response to different changes to the system structure. These simulation models can be used to digitally analyze many real-world systems.

In order to analyze the impacts of different fleet sizes, parking infrastructure, and battery charging strategies on the movement of e-scooters within a fixed geographical area and the ability of the e-scooter fleet to satisfy demand for new trips, a simulation model was required. The simulation model must closely approximate the observed traffic volumes from the available data and the characteristics of each trip while maintaining information about the state of each scooter in the system.

Two simulation softwares were considered as possible foundations for the research of this thesis. SUMO (Simulation of Urban MObility) is an open-source simulation package designed to simulate traffic flows through large vehicular traffic networks [3]. MATSim (Multi Agent Transport Simulation), likewise, is an open-source traffic simulation framework that supports large-scale agent-based simulation models [22]. However, in order to be effectively utilized, these environments would have required more specific data on e-scooter user behaviour and the e-scooter specifications than were contained in the available datasets. By contrast, a custom-built discrete-event simulation environment would allow for more flexibility to focus on the primary research topic using only the available data, while maintaining an appropriate scale, computational load, and ability to accommodate frequent repetition with a varying workload model. This method also benefitted from previous experience working with discrete-event simulation in a similar problem domain (e.g., optimizing transportation for bottle recycling). Moreover, this approach could draw from this existing discrete-event simulation code base which could be modified and reused for the construction of the e-scooter simulation.

2.3.2 EV Battery Models

Because both the ability of the e-scooter fleet to satisfy user demand and the time and distance requirements to collect, recharge, and redistribute scooters are directly tied to the charging and discharging rates for the e-scooter batteries, the development of a robust e-scooter battery model was crucial to the construction of the simulation. This is a familiar problem within the field of EV simulation modelling and consequently there are previous studies that discuss approaches to modelling EV batteries.

As with many aspects of simulation, one of the fundamental challenges in developing a battery model is clearly defining which aspects need to be modelled in detail and which

approximated through abstraction. The principal battery technologies used for EVs are lead acid, nickel metal hydride, lithium ion (li-ion), and sodium nickel hydride [5], with li-ion batteries being the most common battery used for e-scooters. An exact representation of e-scooter batteries would need to account for long-term degradation in capacity and performance resulting from the ambient temperature, the state of charge (SOC), and the frequency with which the battery is charged and discharged [53], as well as the precise dimensions of battery cells and the electrochemical reactions within each cell [17]. However, for large scale simulation in which the e-scooter battery is simply one of the building blocks in one of many moving components, a more efficient model is needed.

A 2014 study simulating the installation of EV battery charging stations in Curitiba, Brazil calculated the energy consumed between battery charging stations as a function of the distance travelled, a penalty factor for traffic between stations, and a scalar variable relating the distance travelled with the energy consumed [45]. A slightly less abstracted model was proposed by Kurczveil, López, & Schnieder which used a mathematical model based on kinematic equations that accounted for air and rolling resistance as well as changes in elevation [26].

2.4 Summary

The rapid adoption of SMMSs is indicative of a cultural shift away from privately owned motor vehicles and towards a more distributed transportation system. This shift carries a great deal of potential to solve problems of traffic congestion, vehicle related CO2 emissions, and create a more complete transportation network in urban centres. However, much work is required to facilitate widespread adoption of SMMSs and to identify and address the new problems of safety and space management that SMMSs present. This process must begin with rigorous analysis of empirical data to develop a thorough understanding of user behaviours and key performance metrics. This analysis is described in Chapter 3.

3 Data Characterization

This chapter describes the data analysis and workload characterization processes. Section 3.1 introduces and contextualizes the datasets to be analyzed. Section 3.2 discusses yearly, daily, and hourly variations in e-scooter traffic volumes. Sections 3.3, 3.4, and 3.5 describe the distributions of trip distance, speed, and duration, respectively. Section 3.6 summarizes the chapter.

3.1 Data Sources

The e-scooter data that was analyzed and used as a basis for the simulation model consisted of a public dataset of e-bike and e-scooter trips in Calgary throughout 2019 [57] and a collection of aggregate data spanning across 2019 and 2020 shared by the City of Calgary. The 2019 trip data consisted of 482,021 data entries of seventeen fields, including: (1) type of vehicle (i.e., bike or scooter) used for the trip; (2) the date on which the trip took place; (3) the hour of the day when the trip was initiated; (4) the day of the week on which the trip took place; (5) the trip distance in metres; (6) the trip duration in seconds; (7) the start and end points of the trip; and (8) the community from which the trip originated. The aggregate data supplied by the city included geographical route and parking information, as well as combined statistics regarding trip volume, distance, and speed, from both 2019 and 2020.

For the purposes of simulation modelling, only scooter trips were included, which reduced the number of trip entries to 464,743. Moreover, the data considered were limited to trips originating within the six Calgary communities that make up the downtown area shown in Figure 3.1, referred to in the City of Calgary data as (1) ‘Beltline’, (2) ‘Downtown Commercial Core’, (3)

‘Downtown West End’, (4) ‘Downtown East Village’, (5) ‘Eau Claire’, and (6) ‘Chinatown’. Isolating for trip origin point further reduced the number of trip entries to 299,924.

Figure 3.1: Calgary communities considered for data analysis [57]

3.2 Trip Volume

The mid-pilot report published by the City of Calgary in 2019 [46] stated that 750 000 e-scooter trips had taken place since the pilot began, with that number rising to a total of 1.9 million e-scooter trips in the final report the following year [47]. During the shared mobility pilot period, the e-scooters were available only in summer and early fall, with the scooters being removed during the winter months. These numbers show a significant increase in ridership between 2019 and 2020 as Calgarians became more familiar with the SMMS being offered. Although the exact number of trips recorded is inconsistent between data sets, suggesting that some trip records may have been filtered out, this increase does appear to be reflected in the aggregate data from 2019 and 2020, with the sum of daily scooter trips rising from 672,853 in 2019 to 950,856 scooter trips in 2020.

While the total trip volume appears to have increased by 40-50% on a year-to year basis, the daily trip volumes, shown in Figure 3.2, are comparable between 2019 and 2020, with daily trip volumes in 2020 occasionally falling below their 2019 counterparts. The counts for 2020 also show much clearer periodicity as a result of differences in weekend and weekday behaviour, as well as a much earlier peak and an earlier accompanying drop-off in ridership than was reported in 2019.

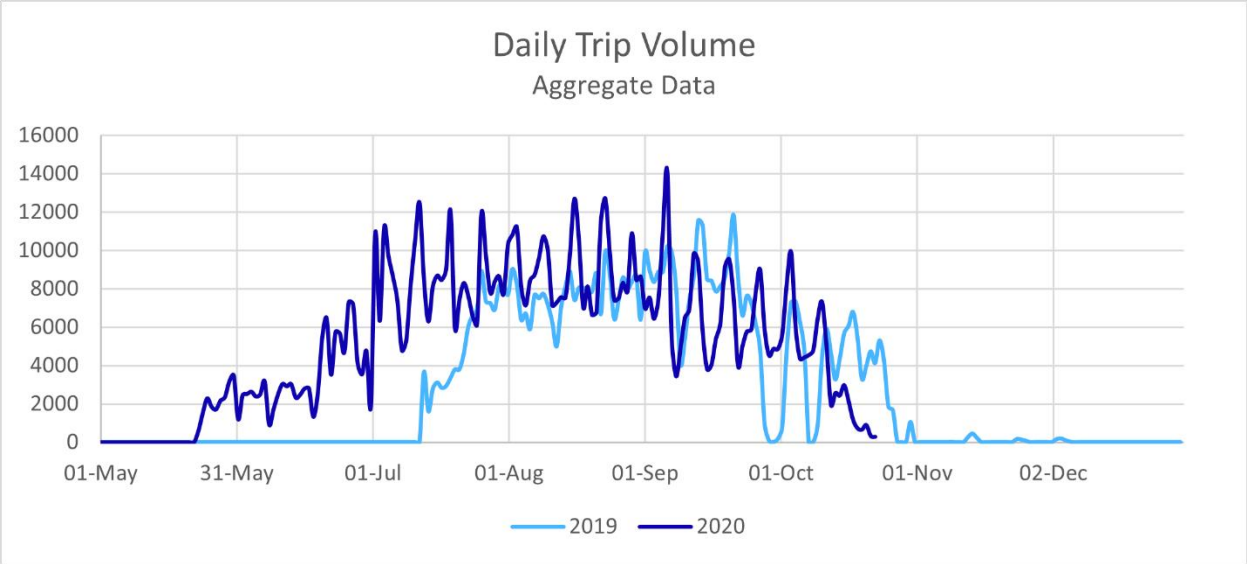

Figure 3.2: Total daily volume of e-scooter trips reported in 2019 and 2020

There are several factors that may have influenced these differences in e-scooter ridership. In 2019, the e-scooters were not made available for use until mid-July, while in 2020 the scooters were made available in limited numbers as early as May, which may account for this earlier peak in traffic volume. The permissible fleet size in 2020 was initially reduced to a total of 450 scooters between May 22nd and June 22nd in an effort to accommodate public health concerns surrounding COVID-19 [47], as reflected by the later increase in traffic volume on June 23rd, 2020. Ultimately, the maximum permissible fleet size was increased to 2,800, a higher value than was used in 2019, which may also have contributed to higher traffic volumes. Finally, traffic volumes appear to decline earlier in the fall and more sharply in 2020 than in 2019, seeming to correspond with the

start of a new academic semester. Since e-scooter usage has often been shown to be higher in areas populated with students [10], [24], this may be related to most post-secondary institutions in Calgary transitioning to online learning in the fall of 2020, reducing the need for students to commute to and from campus.

In both 2019 and 2020, e-scooter activity in Calgary is densely concentrated within the downtown area, with downtown trips accounting for two-thirds of all reported scooter trips. The trip data includes 464,743 scooter trips, 299,925 of which (64.5%) originated from one of the six downtown communities indicated above, while the aggregate data for 2019 reported that approximately 64.3% of scooter trips took place within or between these communities. Although no trip-level data was published for 2020 e-scooter trips, the aggregate data from 2020 showed approximately 67.5% of trips took place within or between these communities.

Neither of the available datasets included sufficiently precise information about trip start times to determine whether new trips arrive according to a particular statistical distribution. However, the available data was sufficient to graph the average hourly trip volumes for 2019 and 2020, shown in Figure 3.3, which reveal specific trends in rider behaviour.

(a)

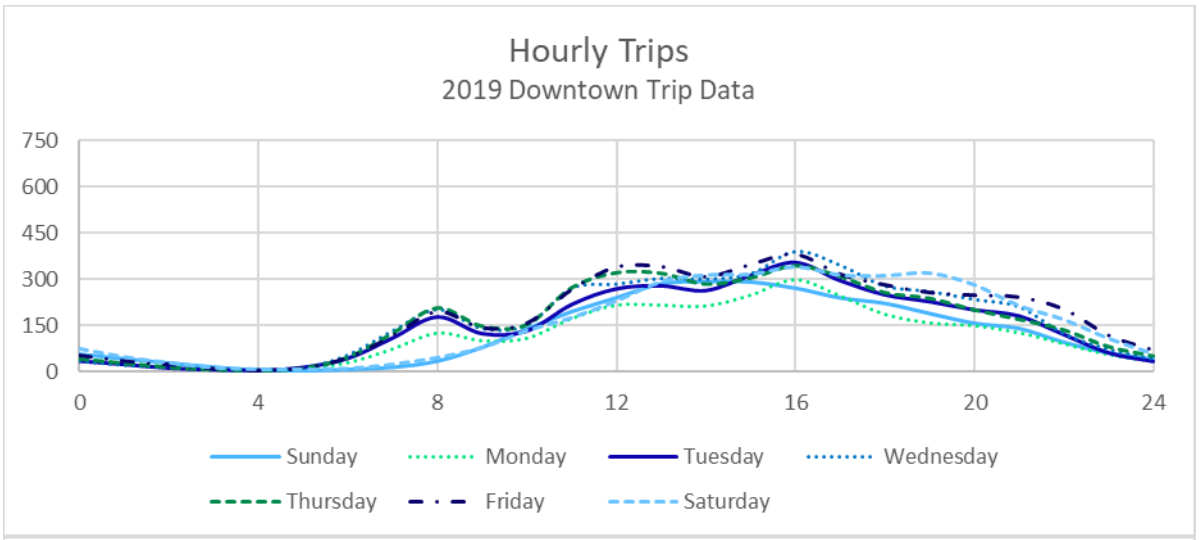

(b)

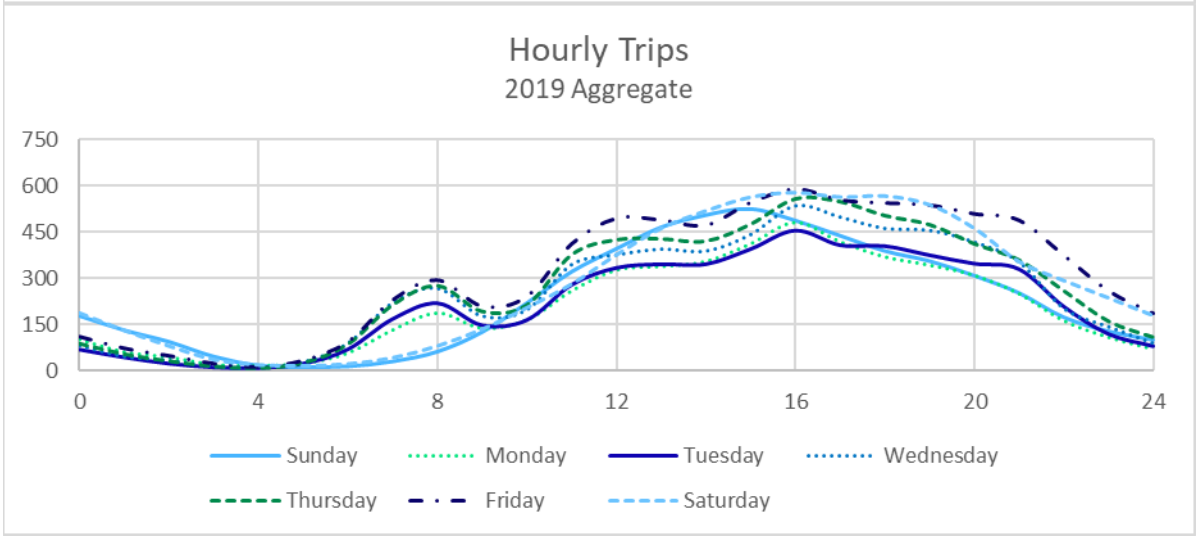

(c)

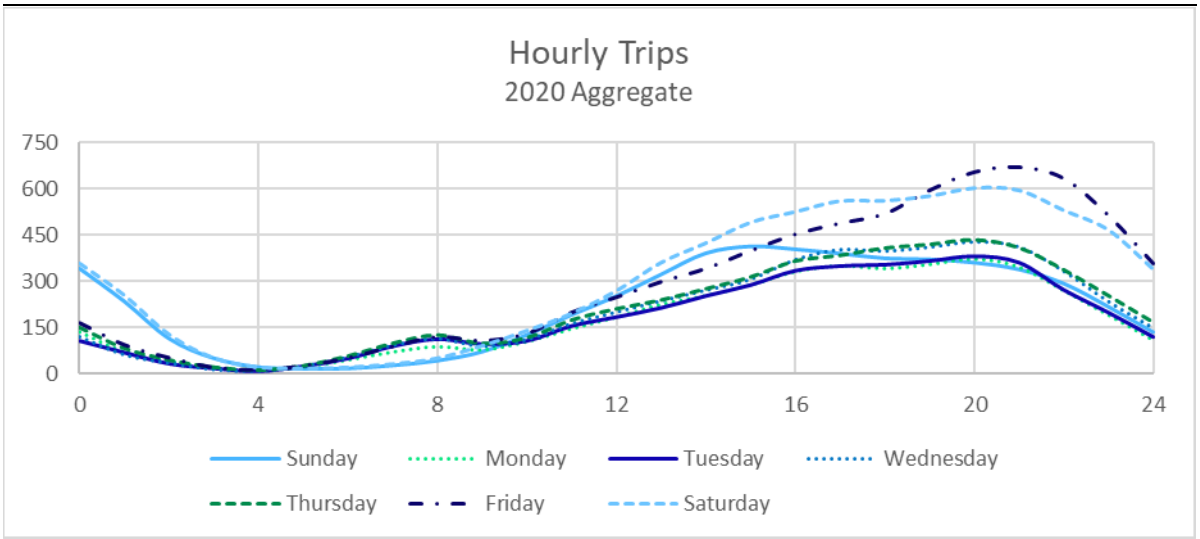

Figure 3.3: Average hourly trip volumes recorded in (a) 2019 trip data isolated to the downtown, (b) 2019 aggregate data, and (c) 2020 aggregate data

Each of these graphs shows a clear diurnal pattern with a distinct lull around 4 AM, and a distinct high in the afternoon or evening. There is also consistently a notable distinction between weekend and weekday ridership patterns, with higher trip volumes on Friday and Saturday evenings and later starts on Saturday and Sunday mornings. However, there are distinct differences in the shapes of these three graphs, particularly with respect to weekday ridership. The 2019 trip data, which has been isolated to the downtown, shows three distinct peaks, at 8 AM (morning rush hour), noon (lunch hour), and 4 PM (evening rush hour) and a slow, steady increase in trip volumes between 4 AM and 4 PM. The 2019 aggregate data shows the same general trends, but the peaks are somewhat less pronounced. This is likely a result of communities outside the downtown being less strictly bound by standard office working hours. Similarly, the traffic volumes are higher because a wider geographical area is considered.

The 2020 aggregate data is starkly different from both of the datasets for 2019. First, the weekday peaks are significantly reduced, with the average traffic volume during the morning rush hour at approximately half the value it reached in 2019, while the peaks at lunch time and evening rush hour have almost vanished. Second, the difference in ridership between weekends and weekdays is substantially more pronounced. In particular, the traffic volumes on Friday and Saturday evenings are higher and do not reach their peak until 9 PM. This is likely attributable to the shift towards telecommuting induced by public health concerns around COVID-19, which would have greatly reduced commuter traffic to and from the downtown.

3.3 Trip Distance

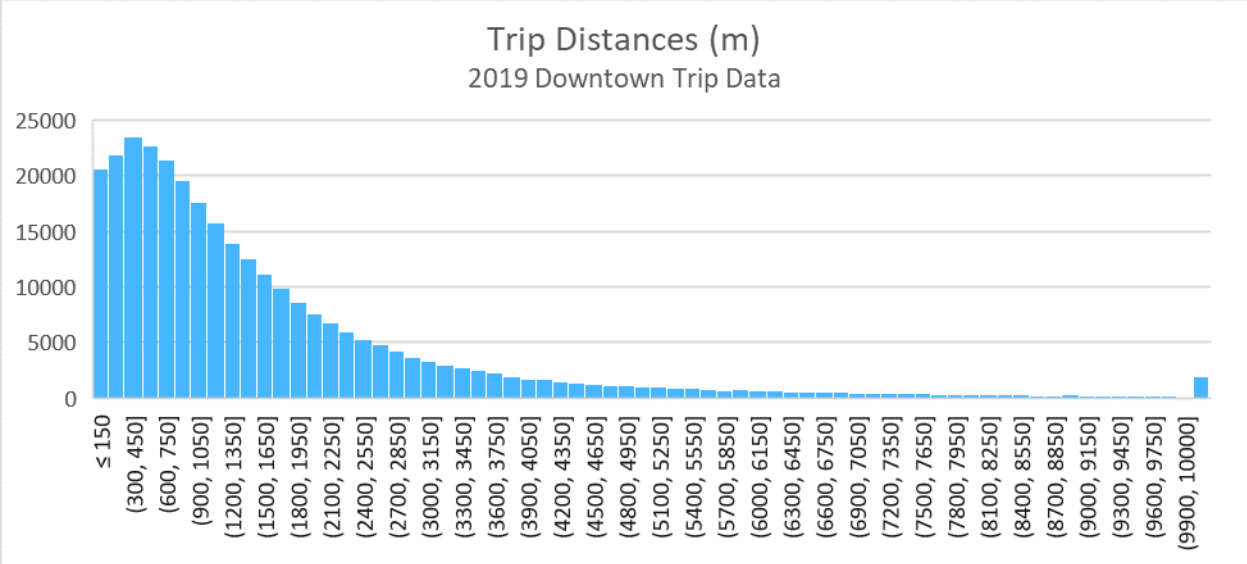

Min	Max	Mean	Median	Mode	Std. Dev	CV
101	27022	1740.112592	1175	642	1818.346795	1.044959277

Figure 3.4: Histogram of observed trip distances in downtown Calgary in 2019

The 2019 trip data included a reported distance in metres for each trip ranging from 0.1 to 27 km. The distribution of trip distances reported in this data set is shown in Figure 3.4. The shape of the histogram suggests that the e-scooter trip distances may follow a lognormal or an exponential distribution. The mean value and standard deviation are similar, as reflected by the coefficient of variation that sits close to one, which is expected of an exponential distribution. However, we have no intuitive explanation for why the trip distances would exhibit the memoryless property that is characteristic of an exponential distribution.

The QQ plots in Figure 3.5 were generated in R [40] using the qqexp() and qqplot() functions. The exponential QQ plot (left) shows a fairly straight line, although the observed distances begin to drift above the expected line towards the tail of the distribution. One common test for comparing statistical distributions is the Kolmogorov-Smirnov (KS) test. This test produces a KS statistic value which quantifies the difference between distributions, with higher statistic

values representing greater deviation between distributions and lower statistic values representing lower deviation between distributions. A KS test of the observed distances against an exponential distribution with a mean value of 1740.112592 produced a KS test statistic of $D = 0.067717$. For a dataset with 299,924 samples, and $\alpha = 0.001$, the critical D value is $\frac{1.94947}{\sqrt{N}} = 0.00355967990195$ which is less than the calculated KS statistic, suggesting that while the distribution of trip distances may be similar to an exponential distribution, particularly in the lower half, the sample distances are not strictly exponentially distributed and have a heavier tail.

Interestingly, because the trip data does not include any trips below 101 metres, a two-sample KS test of the empirical data against a corresponding exponential distribution that has been shifted by 101 produced a KS statistic that, while still not below the critical value, is approximately half that of the original sample set.

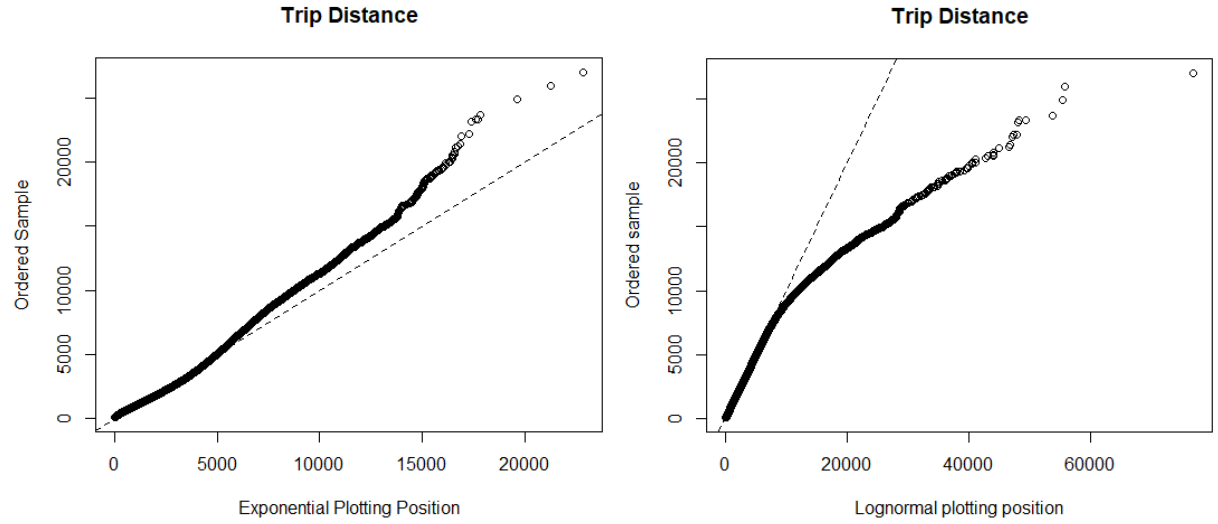

Figure 3.5: QQ plot of observed 2019 trip distances against hypothetical exponential and lognormal distributions

The lognormal QQ plot (right) shows a much closer match in the main body of the distribution but diverges by a more substantial margin at the tail. A KS test of the observed distances against lognormal distribution, fitted using R with a mean log value of 7.03425 and a

standard deviation log value of 0.9486314, produced a KS test statistic of $D = 0.015591$. This value also lies above the critical *D* value, distribution of trip distances does not strictly adhere to a lognormal distribution.

The report of trip distances contained in the aggregate data did not cover as extensive a range as the distances reported in the 2019 trip data, only including a distribution of trip distances ranging from 0 to 5 km. It is unclear whether this distribution reflects rider behaviour from 2019, 2020, or both years together. A graph comparing distance distributions from the aggregate and trip datasets is shown in Figure 3.6. The distributions are closely matched over most intervals, however the trip data from 2019 showed a much smaller percentage of trips under 0.5 km and a much higher percentage of trips over 5 km, resulting in a higher average distance than was reported in the aggregate data.

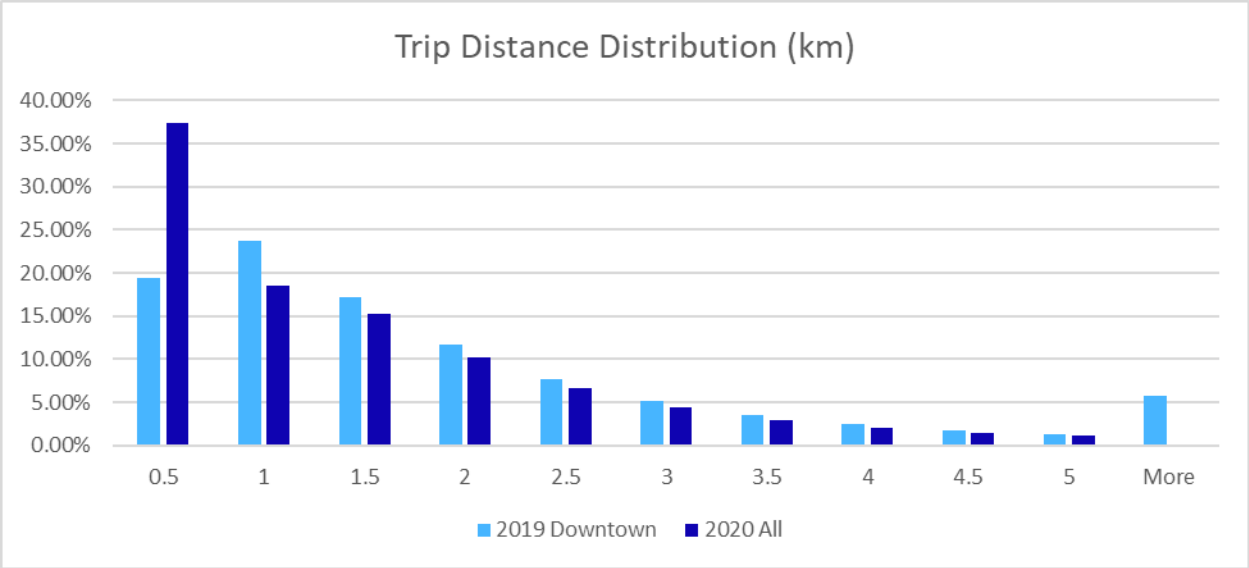

Figure 3.6: Comparison of trip data with the trip distance distribution given in the aggregate data

Additional examination of the hourly variation in trip distances (Figure 3.7) shows that, like trip volume, the distances follow a distinct diurnal pattern, with a slow increase in trip distance throughout the day which quickly falls off between 2 and 6 AM. The hourly trip distances during

this period contain more variation than is present at other times of day, likely due to the lower trip volumes at this time resulting in a smaller sample size and consequently more noise. Interestingly the small, intermittent peaks in this graph appear to fall *between* the rush hour and lunch hour peaks previously observed in the hourly trip volumes, which may reflect a difference in trip purpose (i.e., commuting versus recreation). There is also a clear distinction between weekend and weekday riding behaviour, with early morning and day-time trips being longer on average on weekends than during the week.

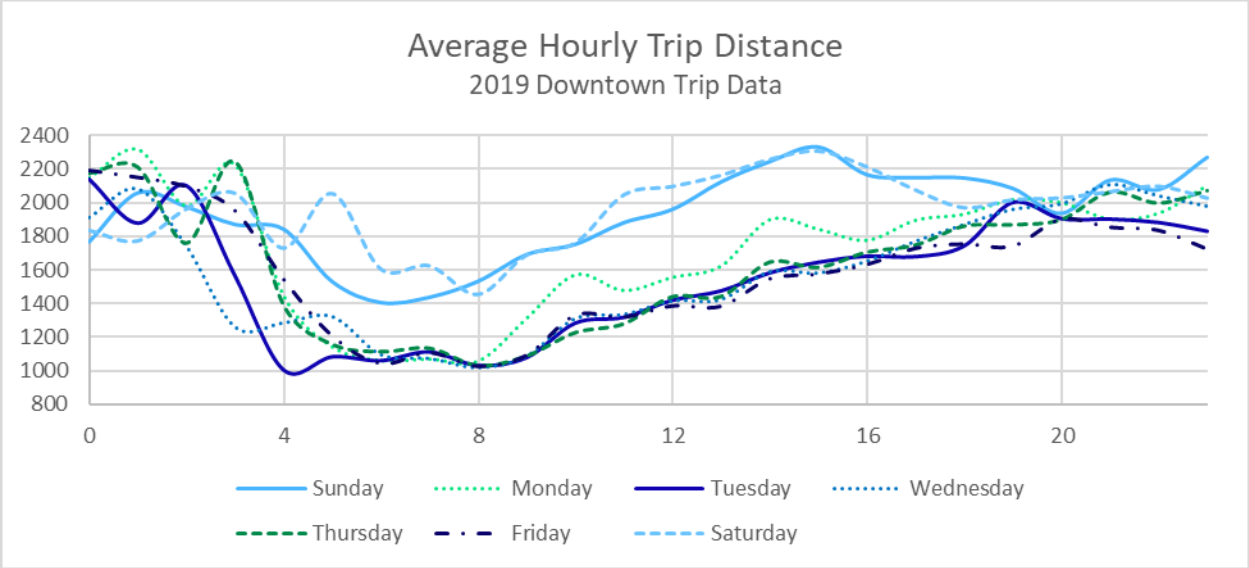

Figure 3.7: Average hourly trip distance observed in 2019

Determining the distribution of trip distances within a given one-hour period posed a challenge, particularly during low traffic periods because of noise resulting from the reduced number of data points. Thus, for the purpose of analyzing hourly trip distance distributions, the trip distances were divided into 24 sets of one-hour intervals, without consideration for weekday/weekend variance. These distributions, shown in Figure 3.8, all appear to follow a similar general shape which, like the combined distance distribution, is visually similar to an exponential distribution. Figure 3.9 shows exponential QQ plots for trip distances over six selected one-hour

intervals. Like the QQ plot shown in Figure 3.5, these plots suggest that the hourly distributions initially follow an exponential distribution before beginning to deviate towards the tail.

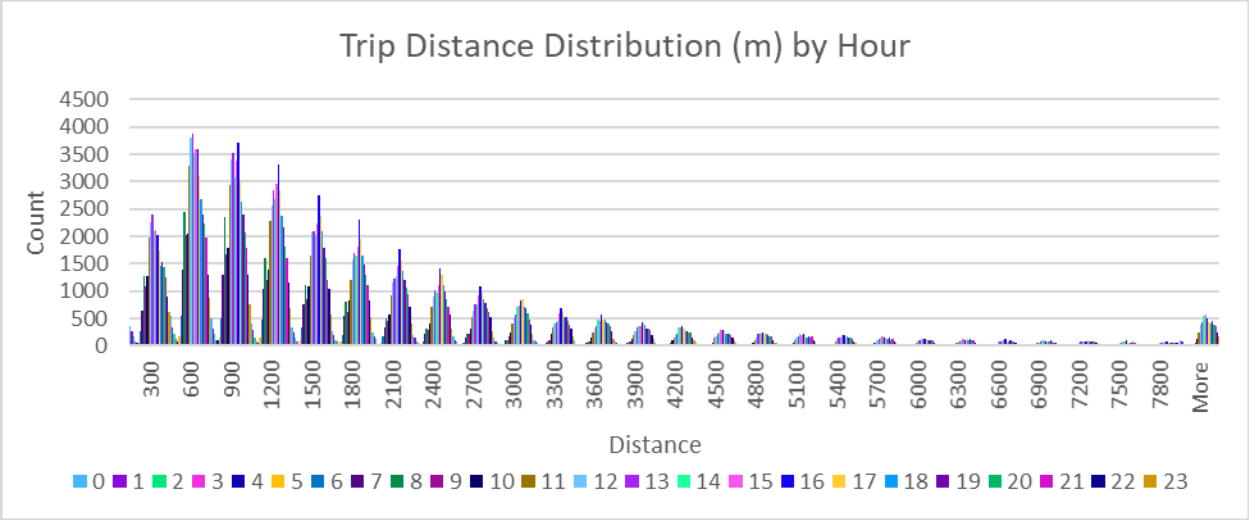

Figure 3.8: Hourly distance distributions

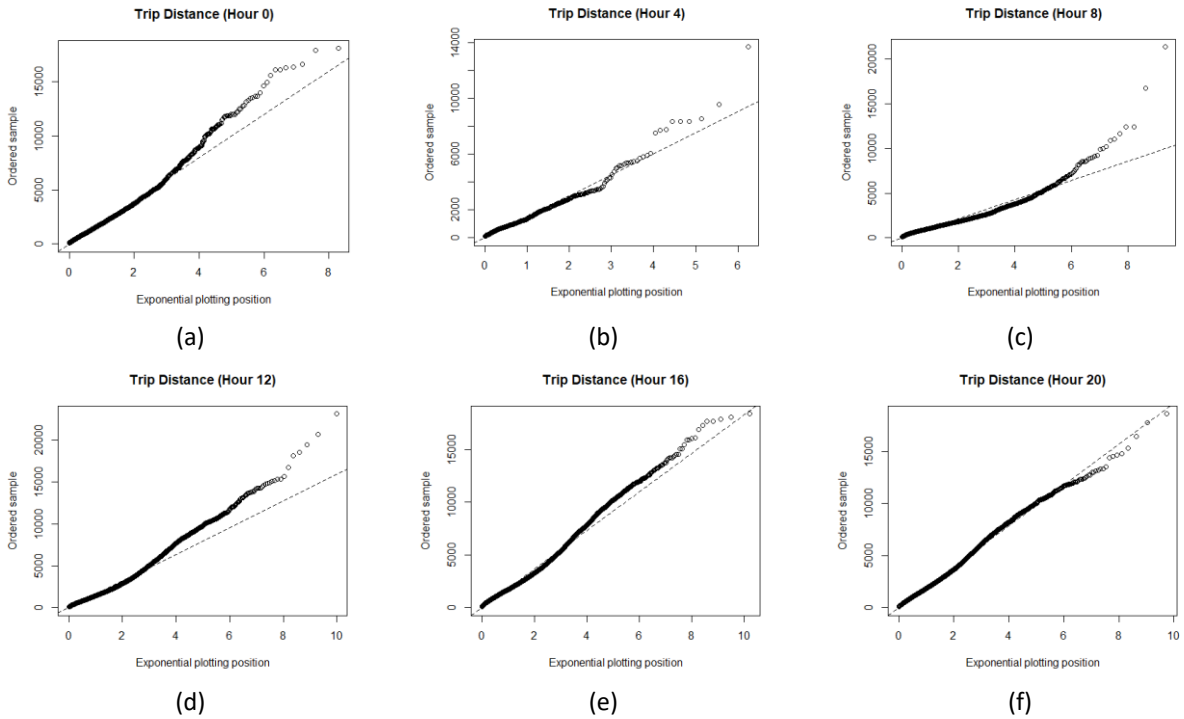

Figure 3.9: QQ plots comparing hourly distance distributions against hypothetical exponential distributions

3.4 Trip Duration

Like the recorded trip distances, the trip durations from the 2019 trip data appear at first glance to follow a distribution similar to a lognormal distribution or an exponential distribution. The distribution of trip durations shown in the histogram in Figure 3.10 is weighted toward the left with a long right tail. Again, the mean and standard deviation are similar, although the coefficient of variation is higher than was seen in the trip distance distribution.

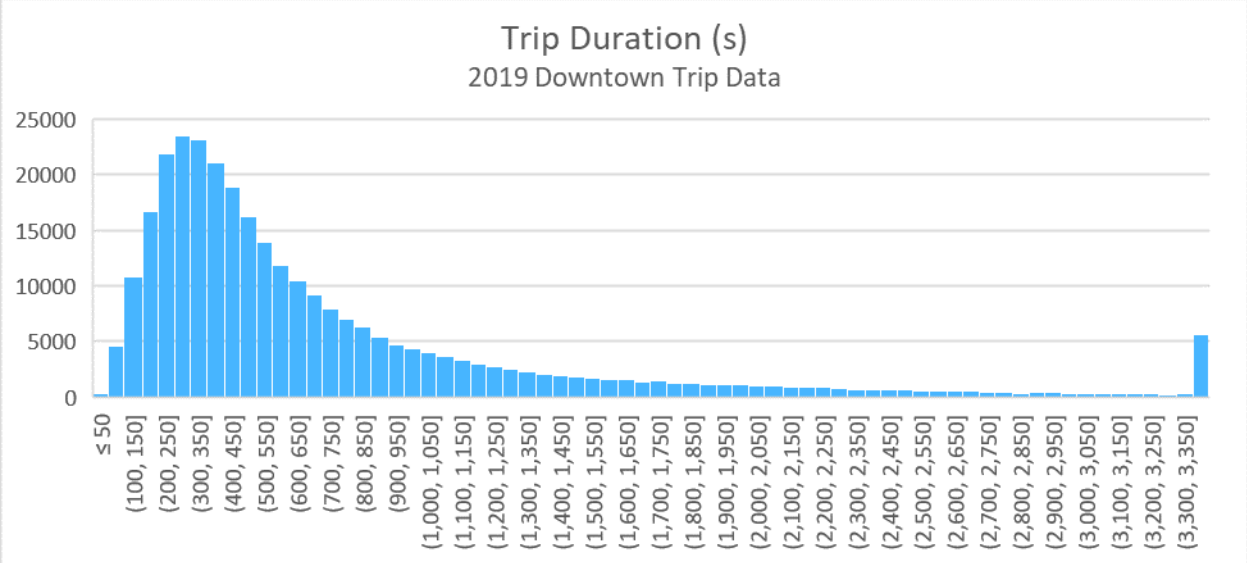

Min	Max	Mean	Median	Mode	Std. Dev	CV
31	9,521	746	476	236	806.5128916	1.081261435

Figure 3.10: Histogram of observed trip durations in downtown Calgary in 2019

However, the QQ plots shown in Figure 3.11 display a sharp divergence from both expected exponential values and expected lognormal values. A KS test comparing the empirical data with a corresponding exponential distribution returns a KS statistic of $D = 0.13256$, rejecting the hypothesis that the trip durations are exponentially distributed. Similarly, a KS test comparing the empirical data with a corresponding lognormal distribution returns a KS statistic of $D = 0.039393$, which while substantially lower than the exponential is still greater than the critical D value. The aggregate data did not include a report of recorded durations for comparison.

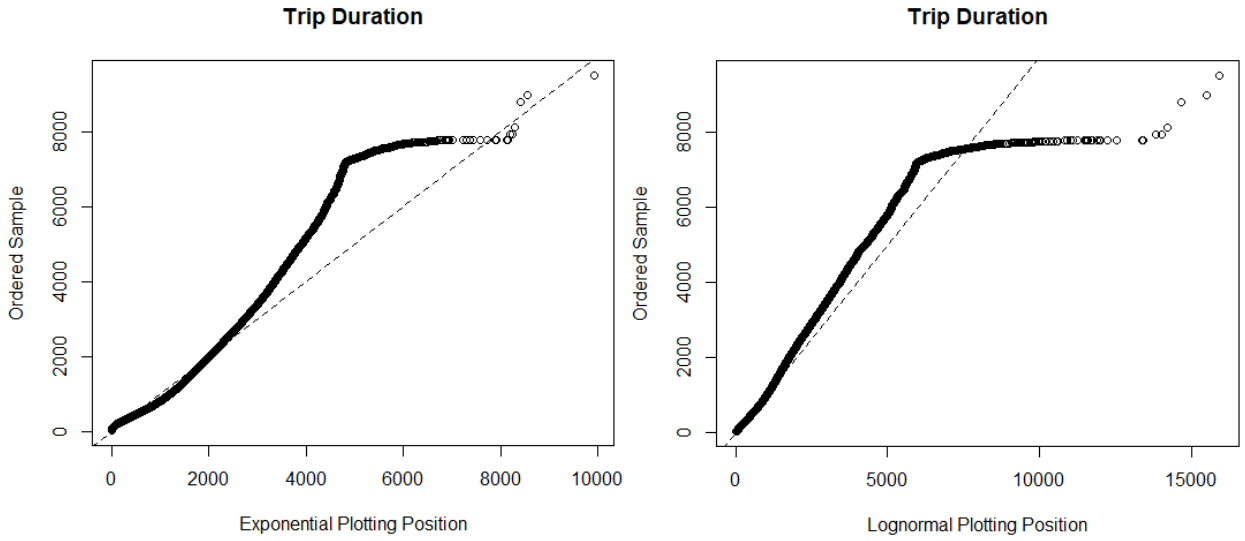

Figure 3.11: QQ plot of observed 2019 trip durations against hypothetical exponential and lognormal distributions

There is no immediately apparent explanation for the unusual behaviour in the tail of the distribution. The hourly distribution of trip durations, given in Figure 3.12, closely matches the hourly distribution of trip distances given in Figure 3.7. A histogram showing the approximate number of trips ending in each hour of the day, given in Figure 3.13, closely matches observed traffic patterns discussed in Section 3.2 without any unusual spikes or lulls.

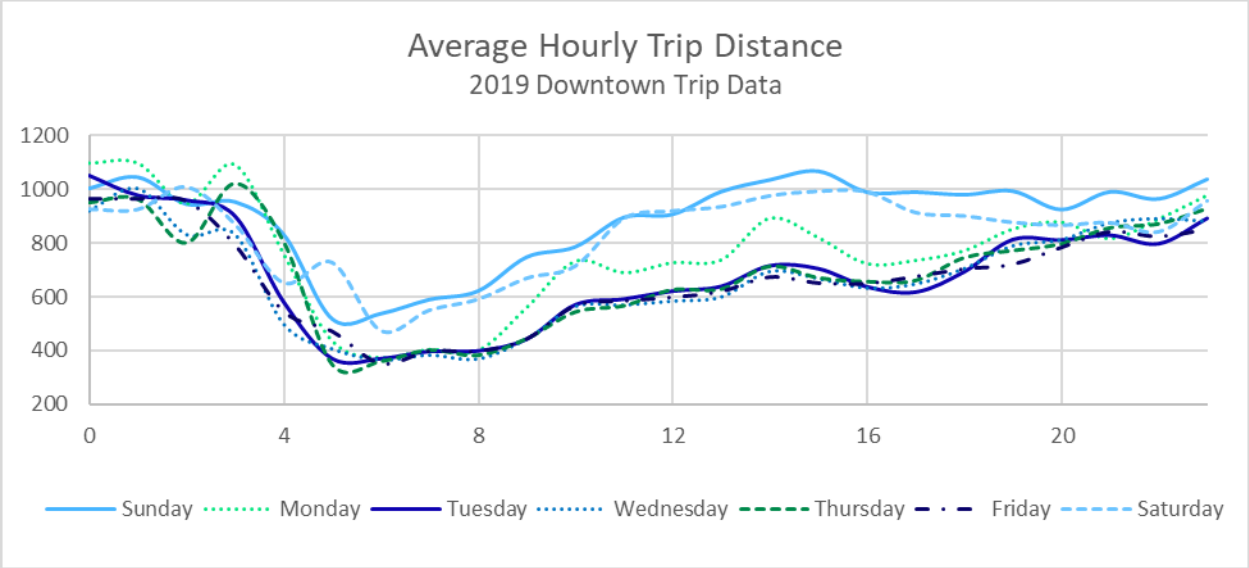

Figure 3.12: Average hourly trip duration observed in 2019

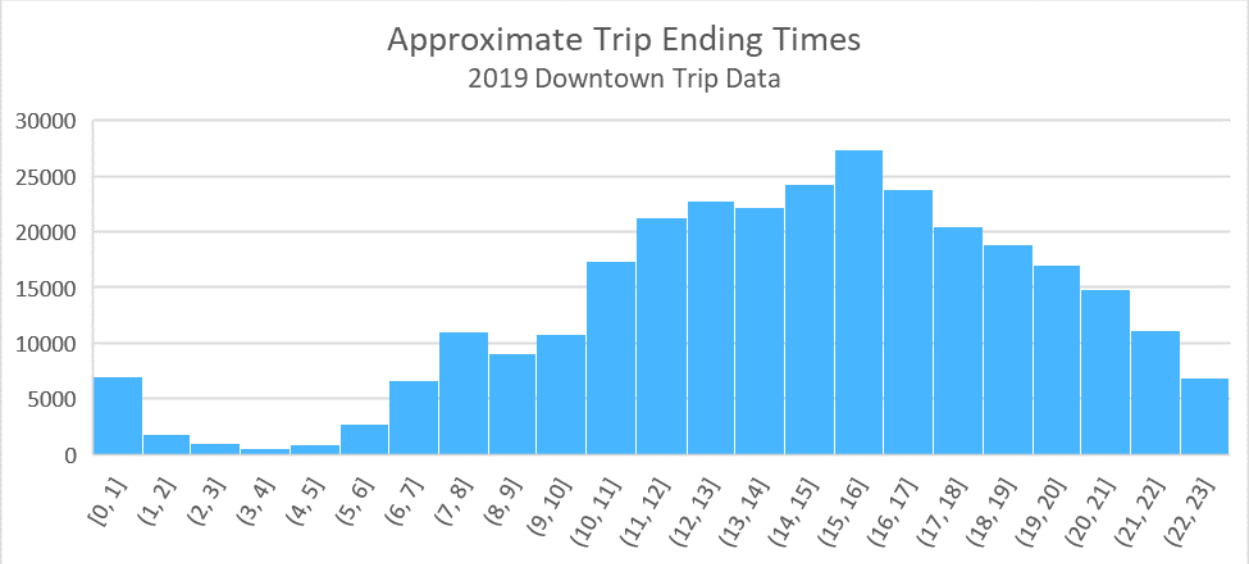

Figure 3.13: Approximate portion of trips ending during each hour of the day

An analysis of the trip durations in comparison with the trip distances appears to show minimal correlation between the two metrics, with one small exception. The scatterplot shown in Figure 3.14, with trip distances represented on the x-axis and trip durations represented on the y-axis, appears to be roughly bounded at the bottom (shown in green) to a maximum speed of approximately 7.5 mps (27 kph), which complies with the typical maximum speed reported for

most commercial scooters[9]. The scatterplot also appears to be bounded at the top, though not strictly, to a maximum duration of 8000 seconds, or 2.2 hours. In fact, there is a dense band (shown in yellow) of points between 7000 and 8000 seconds that stand out from the surrounding plot. This band is consistent with the distinct corner at 7000 seconds that is visible in the QQ plot given in Figure 3.11. Isolating these trip records for further analysis did not reveal any particular trends in the time when these trips took place or their starting and ending locations. Thus, this may be a result of the data collection and filtration processes, or may simply reflect a peculiarity of rider behaviour.

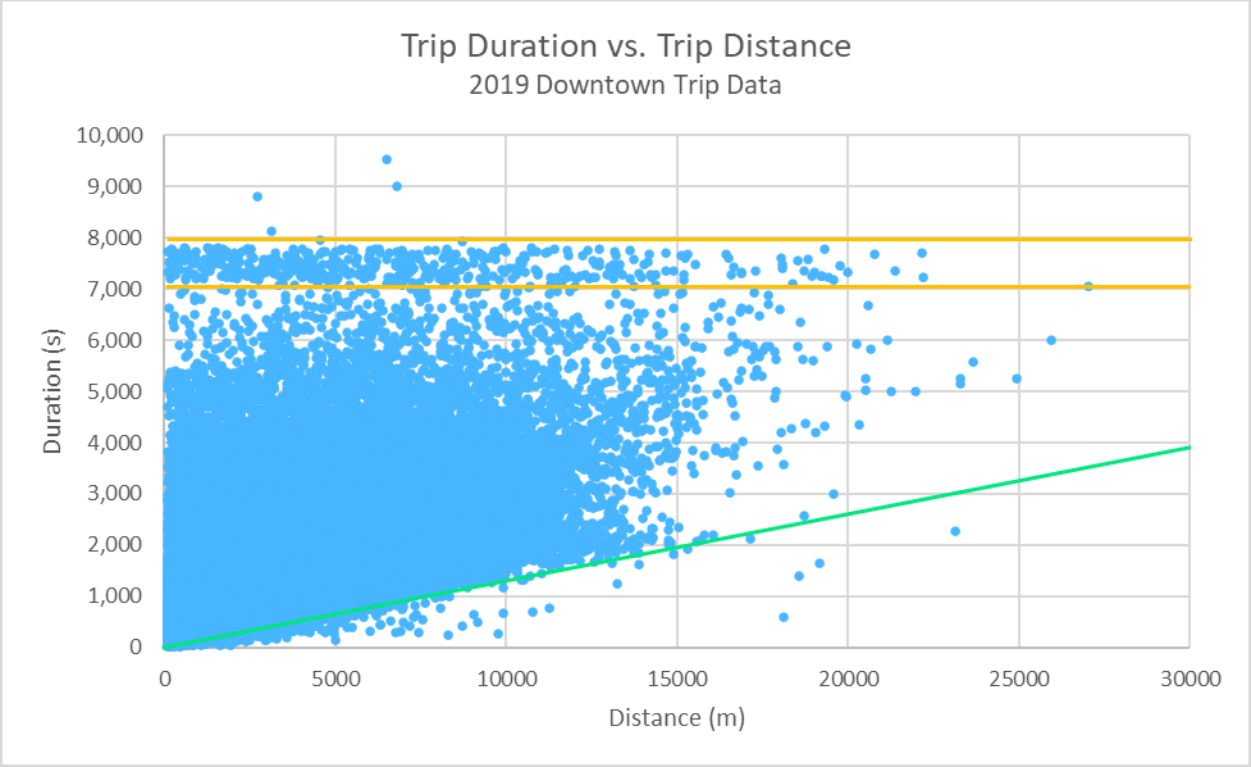

Figure 3.14: Scatterplot of trip distance vs. trip duration in 2019

[9] https://electricscootering.com/electric-scooters-fast/

3.5 Trip Speed

An analysis of trip speed was conducted using the average speed calculated from trip distance and duration. This calculation revealed 792 trip records with a reported average speed of more than 30 kph, with 6 reaching higher than 100 kph. The Segway Ninebot ES4 (Lime's scooter of choice) has a top speed of approximately 30 kph[10] and the ES2 and Xioami Mi M365 have a top speed of approximately 25 kph[11][12]. Since these observed values are beyond the threshold of typical scooter operation, they were presumed to be the result of anomalous user behaviour or errors in data collection and these speeds were excluded from analysis.

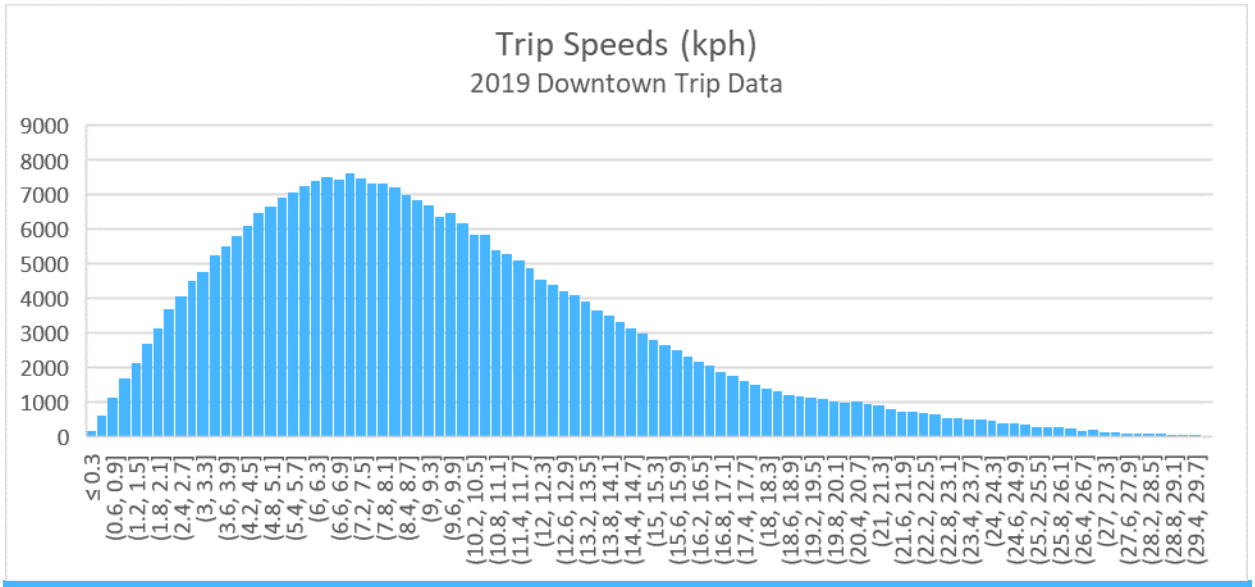

Min	Max	Mean	Median	Mode	Std. Dev.	CV
0.048422142	29.87307692	9.458027784	8.583999998	7.2	5.289484767	0.559258747

Figure 3.15: Histogram of observed trip speeds in 2019

Isolating the data entries with only plausible average speeds gave a mean trip speed of 9.5 kph. Unlike the trip distances and trip durations, the average trip speeds reflected in the 2019 aggregate data do not immediately appear to follow a familiar statistical distribution, and QQ plots

[10] https://www.segway.com/kickscooter-es4/es4-specs/#specs-es4
[11] https://www.segway.com/kickscooter-es2/es2-specs/
[12] https://www.xiaomitoday.com/product/xiaomi-m365-electric-scooter/

comparing the observed speeds against normal, exponential, and chi-squared distributions, given in Figure 3.16, did not yield promising straight-line matches.

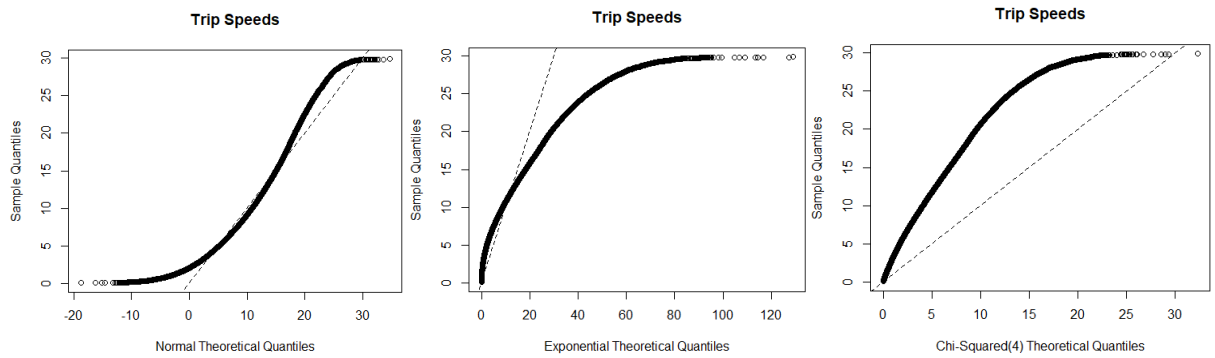

Figure 3.16: QQ plots comparing the observed trip speed distributions against various hypothetical distributions

While the speed values taken from the 2019 trip data represent a simple trip-wise average speed, determined by the reported distance and duration, the aggregate data made available in 2020 does not include information about how the speed data it includes was collected and aggregated, making it difficult to determine precisely what factors contribute to the differences in the two distributions. In particular, the 2020 data is bounded at the bottom to 3 kph and at the top to 14 kph while the speeds from the 2019 trip data vary much more broadly. Even excluding reported trip speeds above 30 kph, these speeds range as low as 0.05 kph and as high as 29.87 kph. One factor that may account for some of the discrepancy between the aggregate and trip data is the 2020 implementation of slow-speed zones in Kensington, Mission, Inglewood, and on Stephen Avenue, which automatically limited the maximum speed of the scooter to 15 kph. A comparison of the two distributions is given in Figure 3.17.

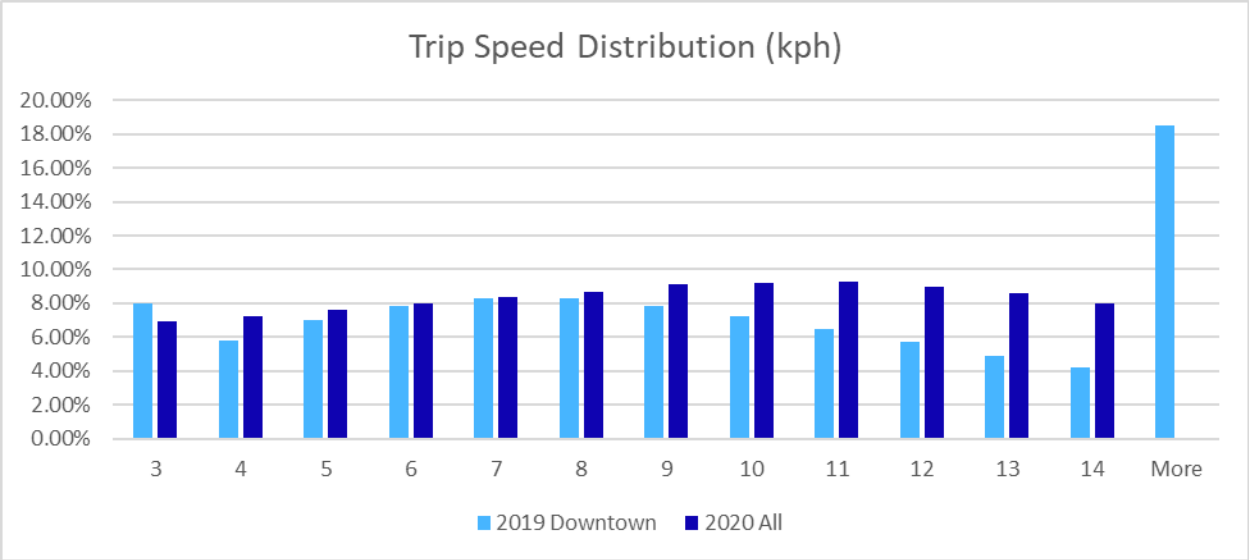

Figure 3.17: Comparison of trip data with the trip speed distribution given in the aggregate data

Finally, an analysis was conducted between trip distance and trip speed, using the 2019 trip data, to look for correlation between the two distributions. The scatterplot given in Figure 3.18 indicates a rather strict lower bound on trip speed as a function of trip distance, shown in yellow. This approximate lower bound may be given as:

$$minSpeed\,\frac{\text{km}}{h} = \frac{tripDistance\ km}{2.2h}. \tag{1}$$

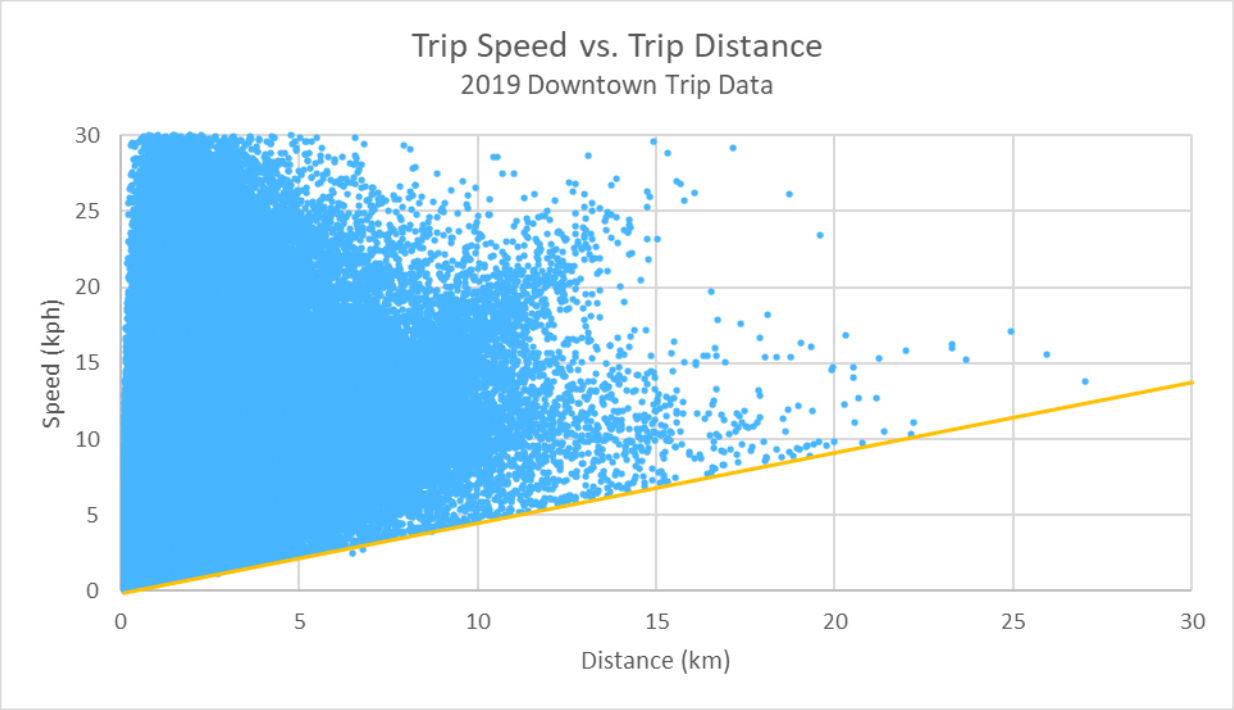

Figure 3.18: Scatterplot comparing observed trip distance and trip speed in 2019

3.6 Summary

This chapter has presented an analysis of two datasets of e-scooter usage in Calgary. The majority of e-scooter trips are concentrated within the downtown area and a temporal analysis of these trip volumes has shown both that e-scooter usage rose between 2019 and 2020 and that there are clearly weekly and diurnal variations in how e-scooters are used. An examination of the trip characteristics showed although neither duration nor speed clearly followed any statistical distribution, the distribution of trip distances was similar to an exponential distribution, though with a heavier tail. These analyses create the foundation for the development of the simulation model discussed in Chapter 4.

4 Simulation Model

This chapter discusses the process of synthetic workload generation and the development of a custom-built simulation environment. Section 4.1 discusses the simplifying assumptions required to represent a complex, real-world system in a finite simulation. Section 4.2 describes the construction and modular structure of the simulation code, as well as the required input variables and output statistics. Section 4.3 describes the process of creating a geographic model for the simulation from the empirical geographic data regarding trip routes. Section 4.4 explains the e-scooter battery model used for the simulation, and how the state of charge (SOC) for each e-scooter battery is determined by e-scooter usage and battery charging time. Section 4.5 discusses the generation of new trips with consideration for hourly variance in traffic volumes, and assignment of trip characteristics including trip distance, trip route, and trip speed. Section 4.6 summarizes the main points of the chapter.

4.1 Abstractions and Assumptions

In the process of transitioning from analysis of real-world data to development of a synthetic workload model, several simplifying assumptions were adopted to maintain the simulation at a manageable scale and reduce computational load, or to accommodate limitations on the available data. Because the daily traffic volumes in both 2019 and 2020 showed a distinct peak in ridership during the summer months compared to a distinct lull in winter, the simulation model focuses on rider behaviour for the months of July and August. In addition, because all datasets showed a clear concentration of e-scooter traffic in the downtown, the simulation geography is restricted to the downtown area, only using GEOJSON map data that falls within the bounding box shown in Figure 4.1.

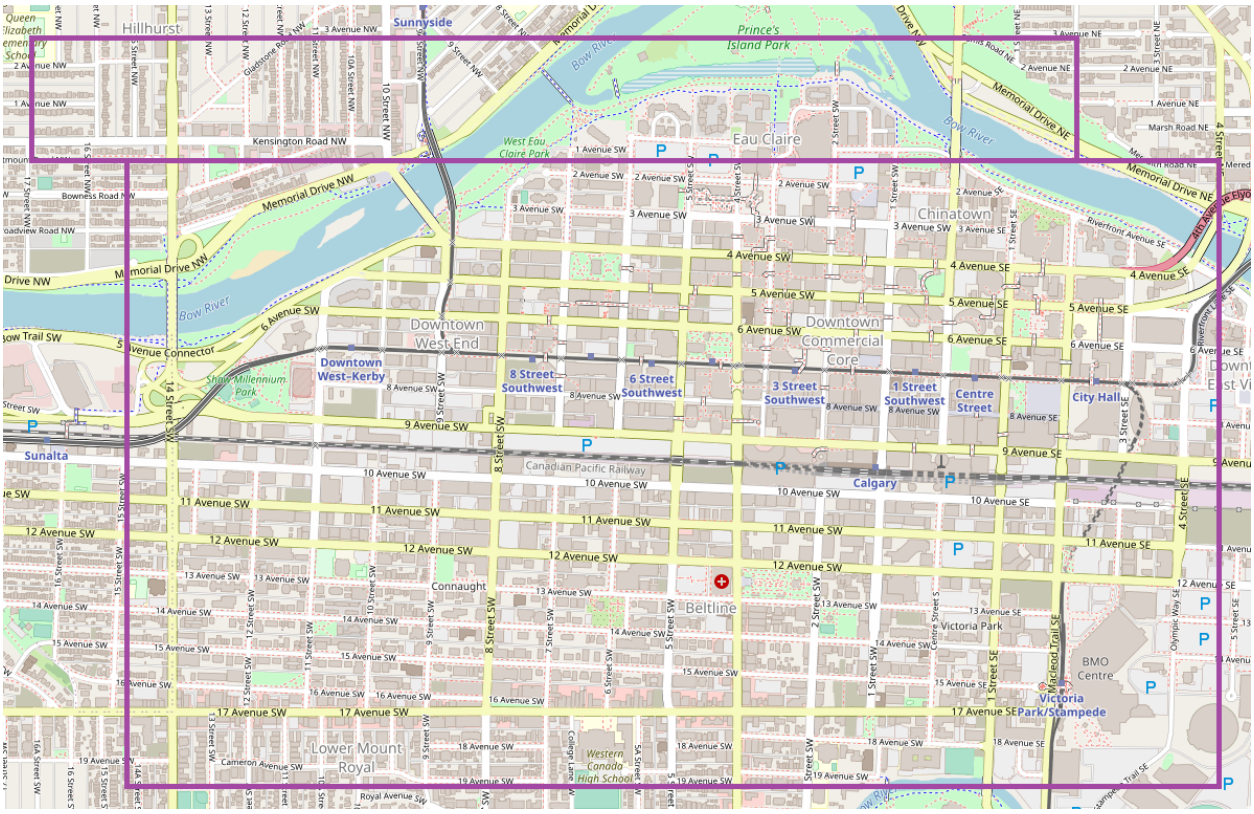

Figure 4.1: Simulation area (© Open Street Map)

In addition to these geographic and temporal limitations on simulation scale, several simplifying assumptions were made about the nature of e-scooter trips and collection strategies. These assumptions include:

- new scooter trips arrive according to a Poisson arrival process, whose rate varies with the hour of the day and the day of the week;
- scooters are selected at random without specific preference for location or charge level, so long as the scooter has sufficient charge to complete a trip;
- no trips are abbreviated by limited scooter battery;
- all e-scooter trips maintain a constant speed between initial acceleration and final deceleration, with no stops or changes in speed; and

- scooters are redistributed to the same point at which they were collected for recharging by the operator.

4.2 Code Structure

The e-scooter simulator was written using the Java programming language [6] and follows the paradigm of discrete-event simulation, whereby the simulation is updated only according to scheduled events that change the state of the simulated system. Designing the simulation this way allows for shorter runtimes of longer simulated periods because the simulation moves directly from one event to the next without having to wait through periods of inactivity, as would be required for continuous simulation using fixed length time steps.

4.2.1 Simulation Classes

The core simulator code is contained in seven Java classes, which have been divided into modules as shown in Figure 4.2.

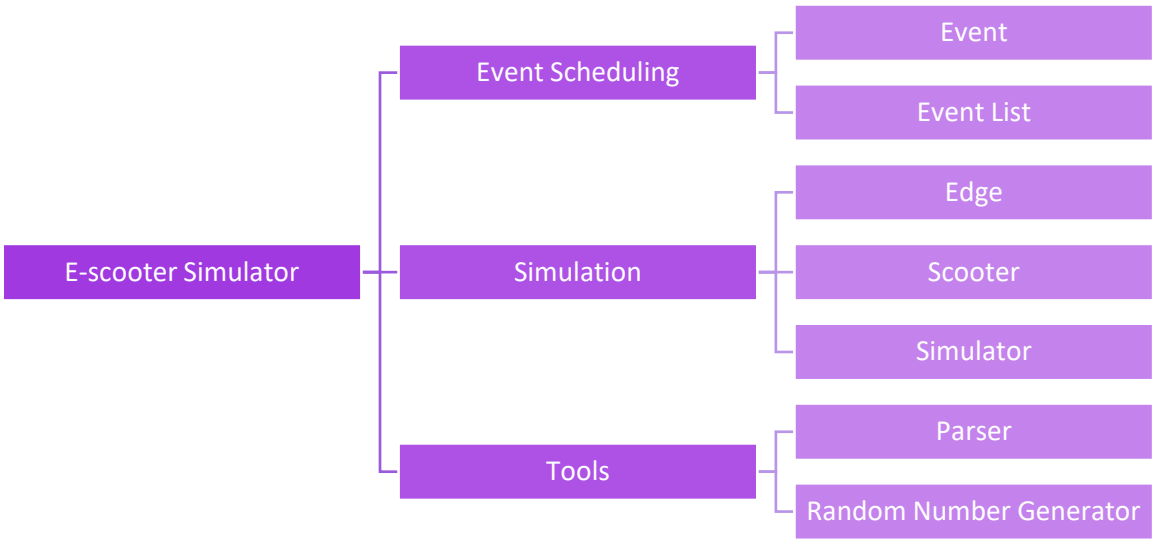

Figure 4.2: Simulation modules and classes

The ‘Event Scheduling’ module contains classes relating to the creation and management of simulated events. The ‘Event’ class stores relevant information about a simulated event including: (1) the time in the simulation when the event occurs, (2) the type of event, and when necessary (3) the scooter and map edge associated with the event. The ‘EventList’ class is a time-ordered linked list of Event objects, so that the earliest upcoming event is at the head of the list and new events are slotted into the list according to the time in the simulation when they are scheduled to occur.

The ‘Simulation’ module contains the simulation code itself, as well as the object classes for the structural and moving components in the simulated e-scooter system. The ‘Scooter’ class includes a unique identifier for the scooter and state variables to keep track of (1) the scooter’s location, (2) the current charge level in the scooter battery, (3) whether the scooter is currently available for use[13], and (4) if parked, whether the scooter is parked at an Share-and-Go (SNG) zone, a battery charging station, or neither. The ‘Edge’ class contains a unique identifier, as well as (1) the distance across the edge, (2) the edge weight, which represent the relative traffic volume across that edge and is used to determine trip routes, (3) the starting and ending coordinates of the edge, and (4) a list of immediately adjacent edges. The primary simulation class includes an event loop that tracks the simulation time and reads new events from the event list until the simulation stop time is reached, as well as event handling functions that update the state of the system and track statistic variables.

[13] A scooter may be unavailable for use if the scooter battery reaches 0, if the scooter has been/is being collected by the operator to be recharged, or if the scooter is already in use by another rider.

Finally, the ‘Tools’ module contains a parser for reading in complex simulation inputs, such as the edge geography for the simulation or the hourly ITTs, and a random number generator for generating ITTs, trip distances, and trip speed.

4.2.2 Inputs and Outputs

The simulation takes four text files as input, as shown in Figure 4.3. These include the edge geography for the simulation, which consists of: an entry for each edge containing the edge length, weight, and neighbours; the mean ITTs in the form of twenty-four rows (hours) of seven columns (days); the mean trip distances in the form of twenty-four rows (hours) of two columns (weekday/weekend); and the empirical distribution for trip speeds between 0 and 30 kph.

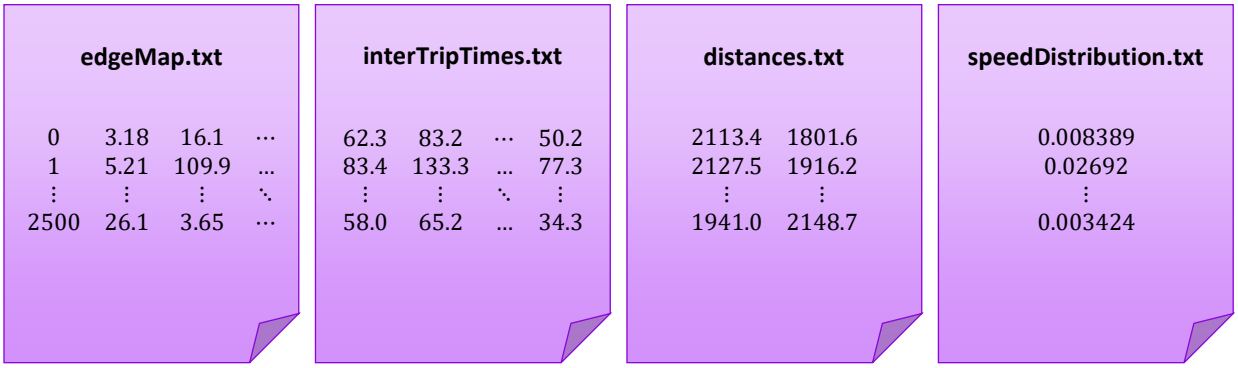

Figure 4.3: Text file simulation inputs

In addition to these inputs, the simulation contains a number of parameters that may be directly modified in the code, including the duration of the simulation, the number of scooters to simulate, the battery percentage threshold below which a scooter will be collected to be recharged, the operator location from which the route for scooter collection originates, and the percent chance of e-scooter riders extending or truncating their trip to find available parking on an adjacent edge. These parameters and their default values or statistical distributions are given in Table 4.1.

Table 4.1: Simulation parameters and default values

Parameter	Default Value	Notes
Number of Scooters	500	N/A
Charging Threshold	25%	N/A
ITT	Exponential(itts[hour][dayOfWeek])	Mean ITTs stored in a 24x7 array
Speed Distribution	Empirical	N/A
Trip Distance	Exponential(distances[hour][weekend?1:0])	Mean distances stored in a 2x7 array
SNG Parking	23 locations with 6 spaces each	Included in the edge geography file

Throughout its runtime, the simulator keeps track of several statistic variables, including (1) the max and mean number of scooters in use at one time, (2) the number of scooter trips both successful and unserved, (3) the number of trips ended at an SNG zone and the number of trips ended at a battery charging station, (4) the average trip distance and duration, and (5) the average time/distance required for an operator to collect scooters with low charge. The simulator also generates a text file that mimics the structure of the 2019 dataset, consisting of start time, day of week, hour of day, distance, duration, and start/end coordinates for each simulated trip.

4.2.3 Events and Event List

Within the scope of this thesis, only four state-changing events were identified as fundamental to the simulation of Calgary's e-scooter system. These events are listed below along with a description of the simulation state changes, statistic variable updates, and subsequent event scheduling triggered by each one.

- *Start Trip:* This event marks the start of a new e-scooter trip and contains no additional information beyond event type and time. An available scooter is selected at random, and a target trip distance and trip speed are generated from their respective stochastic distributions, which in turn determine the percentage of the e-scooter battery consumed by the trip. If the selected scooter does not have sufficient battery to complete a trip of the

length and speed, a new scooter is selected. This process may be repeated up to five times before the trip is counted as unserved.

The origin of the trip is determined by the location of a randomly selected available scooter, rather than the scooter being determined by a randomly selected trip origin. This is because neither of the analyzed data sets contained particularly revealing or precise information about trip start and end points or the general directionality, and because these datasets reflected satisfied demand, where the rider necessarily found an available scooter. If the selected scooter has sufficient battery to complete the trip, a route is generated using the scooter location as an origin point and iteratively extending the route by randomly selecting one new edge at a time, according to their relative traffic volume weights, until the target distance is reached.

Once the scooter, trip speed, trip distance, and route have been determined, the scooter is marked as unavailable because it is in use, any parking or battery charging space the scooter may have occupied is marked as available, and the scooter battery is decremented by the battery consumption of the trip. A record of the trip details is appended to the trip log and the statistic variables relating to distance travelled, trip duration, number of served or unserved trips, and number of scooters in use at one time are updated accordingly. Finally, a new 'End Trip' event for this scooter is scheduled to occur after the determined trip duration at the end to the generated trip route.

Whether or not the trip was successfully served, a new 'Start Trip' event is scheduled according to a Poisson arrival process and the hourly rate of new trips.

- *End Trip:* This event marks the end of a trip and contains additional information about where the trip has ended, and which scooter was used. Because most of the trip details were

determined when the trip was initiated, there is little additional computation that needs to be done at this stage beyond marking the scooter as available again (provided the scooter battery has not reached 0), decrementing the number of scooters in use, and 'parking' the scooter by updating its current location and, where parking or battery charging spaces are available, updating the scooter and edge variables to indicate how it is parked and how many parking or battery charging spaces remain available. No additional events need to be scheduled as a follow up to this type of event.

- *Collect Scooters:* This event occurs once per day at 10 PM and initiates the process of collecting, recharging, and redistributing e-scooters with a low charge level. The threshold for which scooters are considered as having low-charge may be set in the simulation parameters. When this event is triggered, the simulation identifies all the scooters whose battery has fallen below the threshold level, marks each of them as unavailable, and compiles a set of edges with scooters to be collected. Then, with the operator location specified in the simulation parameters as a starting point, the simulation uses Manhattan distance estimation and a modified Shortest Seek Time First algorithm to determine the collection route and the distance driven to collect all the necessary scooters. The time needed to collect these scooters is estimated from the Manhattan distance using an assumed constant speed of 30 kph and with an additional 60 seconds for each edge the collection vehicle must stop at and an additional 30 seconds for each scooter that must be loaded onto the vehicle.

  Since this is a regularly recurring event, a new 'Collect Scooters' event is scheduled for 10 PM the next day. Finally, a new 'Distribute Scooters' event is scheduled to occur after a

period of twice the collection time, plus up to 8 hours or as much time is required to charge all of the scooters to a full battery.

- *Distribute Scooters:* Because the simulation assumes that scooters will be returned to the same location from which they were collected, no additional determinations must be made about the route to distribute scooters or scooter placement. Instead, handling of this event simply requires that each scooter that had been 'collected' for recharging be marked as available with its battery level returned to 100%.

In addition to these four events, a bookkeeping 'Update Time' event is scheduled to occur at the top of every hour to keep track of the current hour (between 0 and 23), the current day of the week (between 0 and 6), and the current day of the simulation, in order to maintain the correct mean ITT and mean distance.

4.3 Geographic Model

The aggregate data included several GEOJSON files mapping aggregate route data along streets and pathways. These files were used to create an edge graph in the simulation, with each edge representing a city street or alleyway, and weighted according to relative daily trip volume across that edge. The data contained in these files included total number of trips observed across that edge and the average number of trips per day as well as latitude and longitude coordinates describing each edge. The starting and ending coordinates of each edge were used to define a simplified simulation geography that ignored curved streets and to identify a list of neighbouring edges for each edge. The aggregate data did not include information about the origin or destination points of individual trips, and the origin and destination points included in the trip data from 2019 were not at a sufficiently fine granularity to make specific observations about the general

directionality of traffic throughout the day. Thus, the route for each e-scooter trip was determined instead by the location of the e-scooter and the relative daily traffic volumes of the surrounding edges.

(a)

(b)

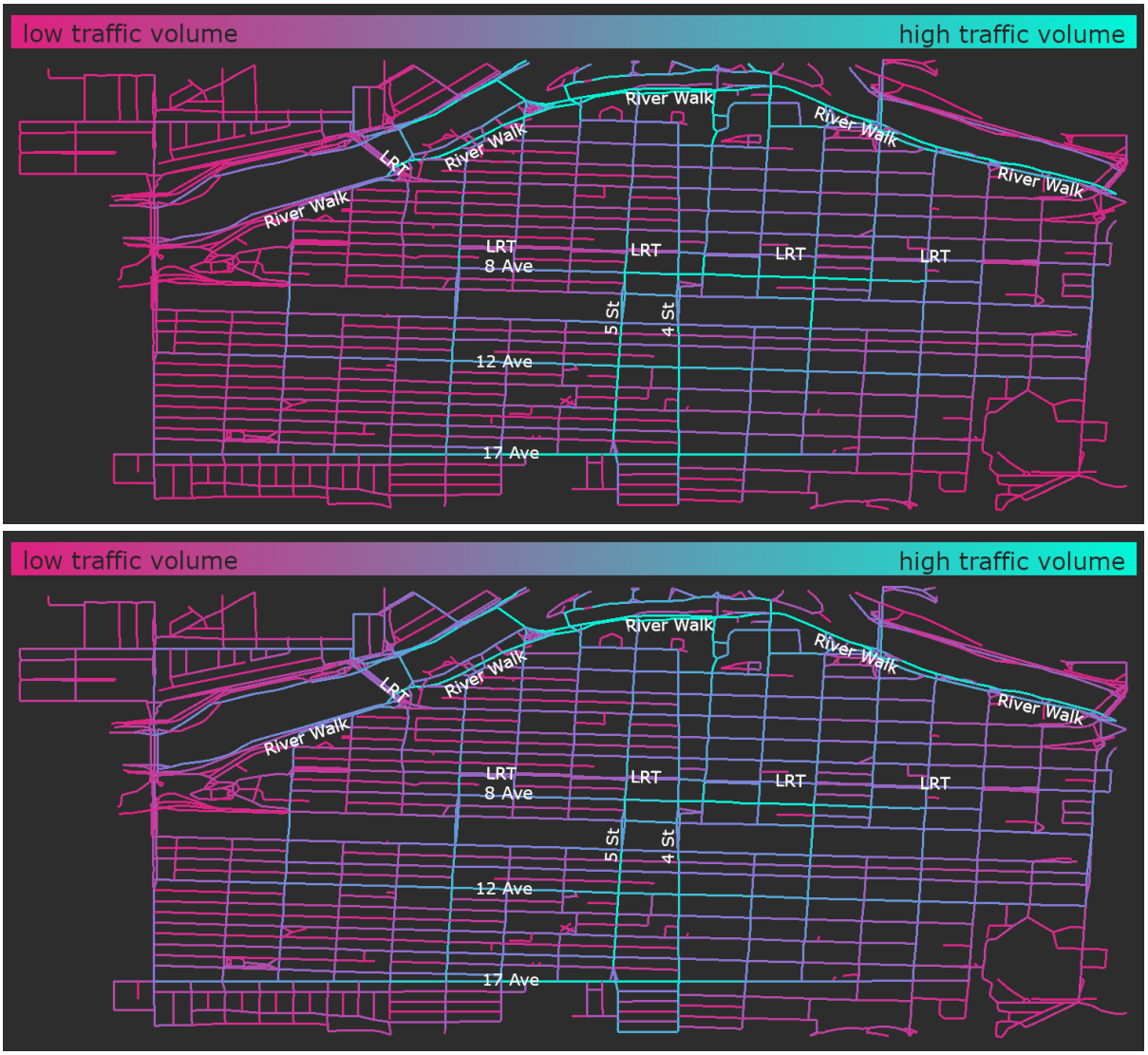

Figure 4.4: Generated maps from (a) observed daily average trips across edge, and (b) simulated daily average trips across edge.

Figure 4.4(a) shows the geographic distribution of average daily traffic volume throughout the downtown as reported in the aggregate data. The map shows several distinct concentrations of traffic, particularly along the River Walk on the north edge of the downtown, but also along the pedestrian road of Stephen Avenue (8th Avenue, one block south of the downtown LRT line) as

well as 12th Avenue and 17th Avenue. In addition, 4th Street and 5th Street, which are two of the main north-south routes across the Canadian Pacific Railway line that bisects the downtown, show a clear concentration of e-scooter traffic. Beyond these specific high-traffic areas, there is a general gradient in traffic volumes that is highest in the eastern-centre of the downtown and gradually decreases towards the edges of the map.

The traffic patterns generated in the simulation using these weights to select trip routes are shown in Figure 4.4(b). In comparison, the simulated traffic closely matches observed traffic in most areas but shows generally more distributed traffic with slightly higher traffic volumes between high traffic streets than is seen in the empirical data.

4.4 E-Scooter Battery Model

4.4.1 Battery Usage

Because the scooters are battery-powered, a robust model for battery charging and discharging behaviour was developed to determine SOC for e-scooter objects within the simulation environment. The fidelity of this model was important, because the rate of charge and discharge would directly impact both the availability of e-scooters for riders and the costs to the operator of collecting and recharging the depleted e-scooters.

The method for calculating e-scooter battery usage is based on the EV battery models in SUMO [26], which derives the equations for battery usage over discrete time intervals, *k*, from kinematic equations. Here E_{batt} (Equations 1 and 2) is the energy stored within the scooter battery, E_{gain} (Equation 4) is the energy gained by the battery between time steps, and E_{veh} (Equation 5) is the energy contained within the scooter motor. Because the geographical map of the downtown is assumed to be flat with no changes in elevation, and because the mass of a scooter is substantially

lower than the mass of an electric car, E_{veh} is determined only by kinetic energy while the potential and rotational energy are ignored. Equations 6 through 8 describe energy lost to wind and rolling resistance. The calculation uses Equation 2 when energy gained by the battery is positive (i.e., when the scooter is decelerating) and Equation 3 when the energy gained by the battery is negative (i.e., when the scooter is accelerating or maintaining constant speed):

$$E_{batt}[k+1] = E_{batt}[k] + \Delta E_{gain}[k+1] \cdot \eta_{recup} \tag{2}$$

$$E_{batt}[k+1] = E_{batt}[k] + \Delta E_{gain}[k+1] \cdot \eta_{prop}^{-1} \tag{3}$$

$$\Delta E_{gain}[k] = E_{veh}[k] - E_{veh}[k+1] - \Delta E_{loss}[k] \tag{4}$$

$$E_{veh}[k] = E_{kin}[k] + E_{pot}[k] + E_{rot}[k] \tag{5}$$

$$E_{loss}[k] = \Delta E_{air}[k] + \Delta E_{roll}[k] \tag{6}$$

$$\Delta E_{air}[k] = \frac{1}{2}\rho_{air} \cdot A_{veh} \cdot c_w \cdot v^2[k] \cdot |\Delta s[k]| \tag{7}$$

$$\Delta E_{roll}[k] = c_{roll} \cdot m_{veh} \cdot g \cdot |\Delta s[k]|. \tag{8}$$

The primary scooter specifications are taken from the published specifications for the Segway Ninebot Kickscooter ES4[14] which is one of the scooters used by Lime. This scooter has two batteries with a combined total of 374 Wh of power, or approximately 1350 kJ. The specifications also claim a typical range of 45 km and a top speed of 30 kph. Some calibration of vehicle acceleration and efficiency was conducted based on these specifications to try and match the range as closely as possible. The final values used for the battery model, and their justifications, are given in Table 4.2.

[14] https://www.segway.com/kickscooter-es4/es4-specs/#specs-es4

Table 4.2: Symbols and values used in battery usage equations

Symbol	Meaning	Value	Justification
η_{prop}	Propulsion Efficiency	0.8	Most EVs report a propulsion efficiency of 0.85-0.9. Accounting for variation and less than ideal conditions, the simulation uses a slightly lower value.
η_{recup}	Regenerative Braking Efficiency	0.01	Although many e-scooters offer regenerative braking, it is frequently inefficient and does not slow down the scooter as quickly as other braking methods. This value gave the best match to the maximum range of a Segway Ninebot ES4
ρ_{air}	Air Density	1.225	Standard
A_{veh}	Drag Area	0.875 m^2	This value is the average height of a Canadian adult (1.7 m) multiplied by the approximate width of an average adult (0.5 m)
c_w	Drag Coefficient	1.2	The drag coefficient of a standing human falls between 1.0 and 1.3
c_{roll}	Rolling Resistance Coeffecicent	0.008	Bicycle tires range from 0.004 to 0.008; solid tires tend to have a higher c_{roll}
m	Mass	94 kg	Mass of an average adult human is ~80 kg; mass of an average scooter is ~14 kg
g	Gravity	9.81 m/s^2	Standard

4.4.2 Battery Charging

Estimating the battery charging time of the scooters was a challenge, particularly with respect to the implementation of public battery charging stations where scooters may be charged for a short period of time rather than a full charging cycle from 0% to 100%. The ES4 scooter, described above, includes a battery charging time of 7 hours in its specifications, while the Bird One scooter[15] used by Bird can take up to 12 hours to charge. One of the factors that further complicates this issue is that EV batteries frequently do not charge at a constant rate. Rather, the rate of charge tends to vary depending on the charge level of the battery.

Ultimately a fixed battery charging time of 8 hours was chosen, based on correspondence with Spin, a scooter company that offers public battery charging hubs for e-scooters. This battery charging model assumes two linear charging functions, requiring three hours to charge a scooter battery from 0% to 50% and an additional five hours to charge a scooter battery from 50% to 100%.

[15] https://support.bird.co/hc/en-us/articles/360040173312-Bird-One-Specs-FAQs-

4.5 Trip Generation

New trips within the simulation were generated according to a Poisson arrival process determined from the average number of hourly trips observed in the 2019 trip statistics. This process uses a mean inter-trip time (ITT) and a uniform random value between 0 and 1 to generate a random ITT according to an inverse exponential CDF, as shown in Equation 9:

$$v = -\mu \ln u \,. \tag{9}$$

However, it was clear from comparison of the total trip volumes in 2019 and 2020 that these values would need to be scaled to better reflect the activity of e-scooter users in 2020. To address this issue, a scalar modifier of 1.55 was introduced to increase the trip volume generated for one simulated month of traffic to 67.5% of the total trip volume reported for July 2020 in the 2020 aggregate data, or the approximate trip volume observed in the downtown area throughout that period. Figure 4.5 shows the average hourly trip volumes observed in downtown Calgary in 2019 (left) side by side with the average hourly trip volumes generated in one month of simulated e-scooters with the 1.55 scaling factor. The simulated traffic captures the diurnal patterns observed in 2019, as well as the distinct tri-peaked shaped of weekday traffic and the later rise in traffic volumes on weekends.

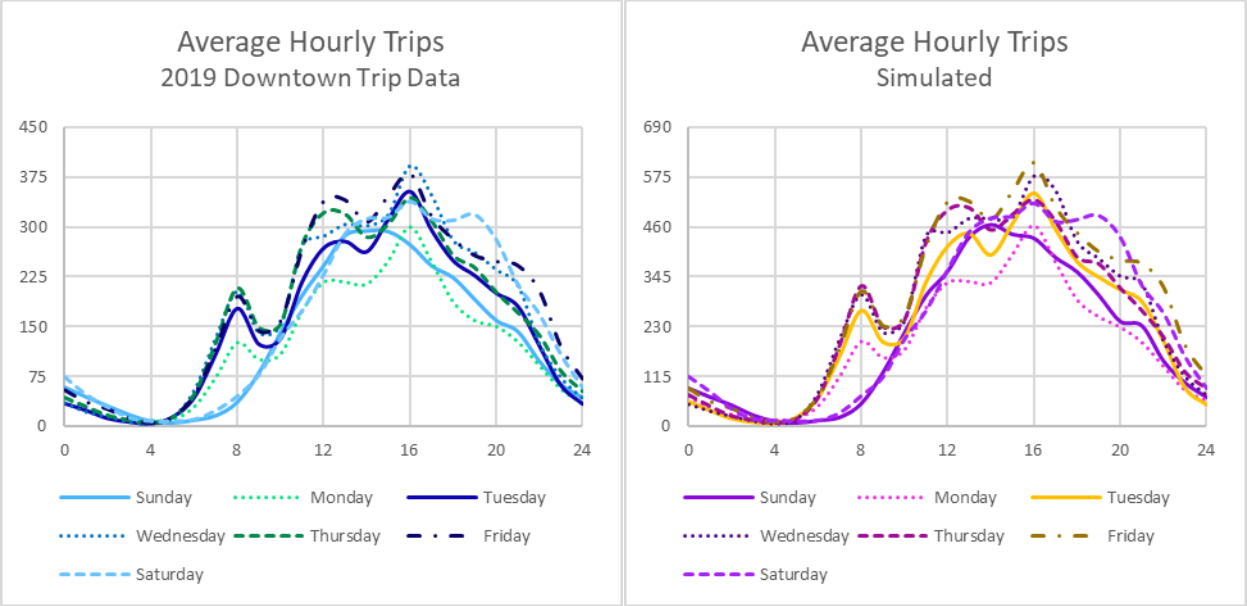

Figure 4.5: Average hourly trip volume in 2019 (left) and simulated hourly trip volume with scalar modifier to match 2020 traffic volumes (right)

4.5.1 Distance

As discussed in Chapter 3, the observed trip distances do not strictly fit an exponential or lognormal distribution. However, because the exponential distribution showed less significant deviation in the lower half of the distribution and because the use of a standardized distribution that is simple to emulate allowed the temporal variation in trip distances to be modelled more efficiently, the trip distances in the simulation are generated according to a shifted exponential distribution, as shown in Equation 10:

$$v = -(\mu - 101)\ln u + 101. \quad (10)$$

Generating simulated distances using this method resulted in an average difference between the observed trip distances and trip distances generated according to a corresponding exponential distribution with a lower bound of 101 metres was only 85.7 metres (slightly less than an average city block in downtown Calgary).

From there, several possible implementations were considered to most accurately reflect hourly, daily, and overall variation in trip distances without introducing undue noise into the system from using too small a sample set. The options considered included drawing random trip distances from:

(a) a single exponential distribution using the overall mean value from the observed trip distances, irrespective of the current day or hour;

(b) one of four possible exponential distributions, using the mean values for weekday peak, weekday off-peak, weekend peak, and weekend off-peak trip distances;

(c) one of twenty-four possible exponential distributions, using the mean hourly values from the observed trip distances, and a uniform scalar value to account for differences in weekday and weekend rider behaviour; or

(d) one of forty-eight possible exponential distributions, using the weekday and weekend mean hourly values from the observed trip distances.

A comparison of the simulated trip distances using the four different methods is shown in Figure 4.6, with the empirically observed hourly trip distances for reference. The fourth distance generation method (d) clearly gives the closest visual match to the observed values, without adding significant noise or noticeable computation time to the simulation process.

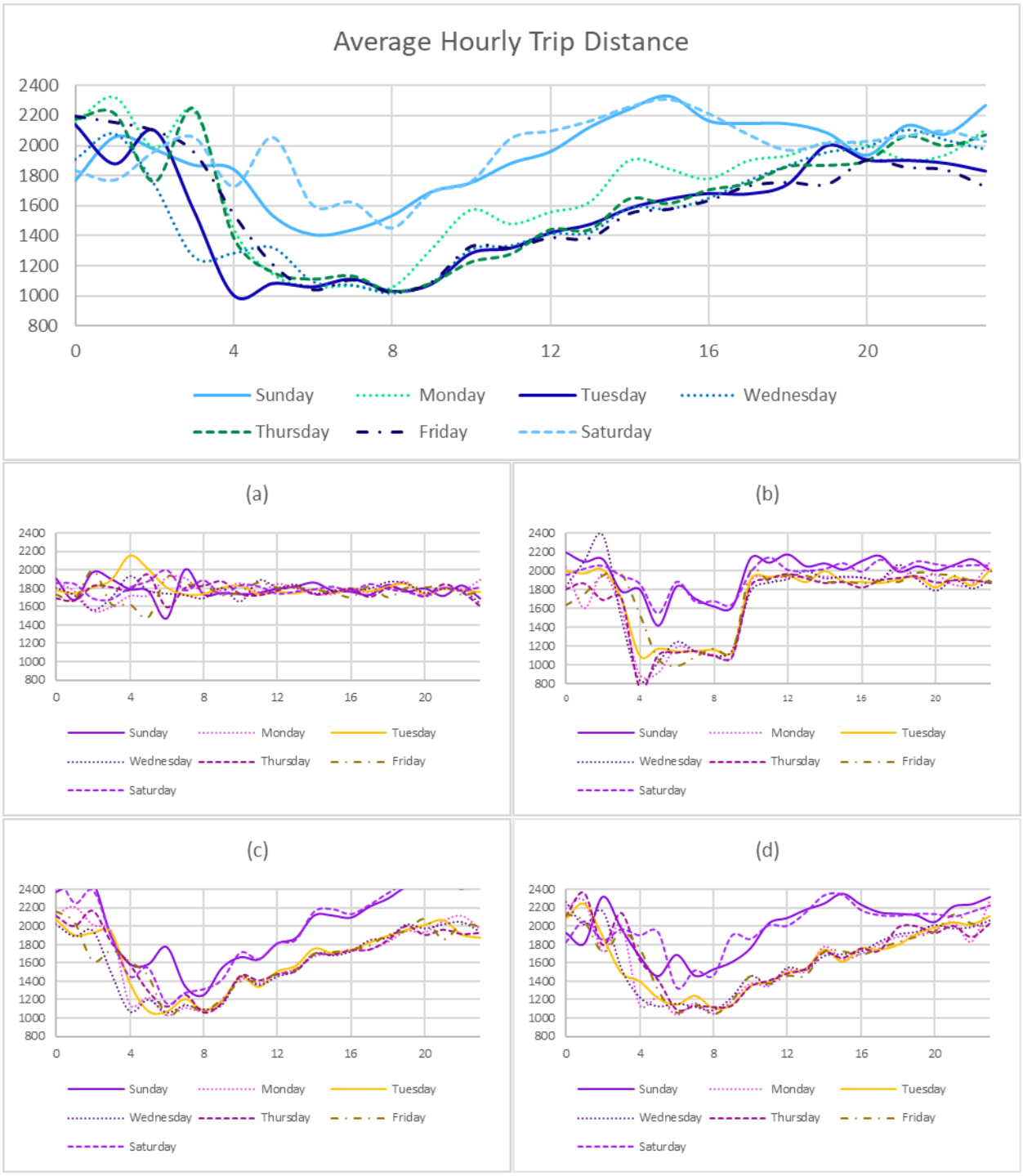

Figure 4.6: Four possible approaches to modelling trip distance

A combined histogram showing the distribution of trip distances in the simulated trip log and the distribution of trip distances in the observed 2019 trip data is given in Figure 4.7, along with a QQ plot comparing the two distributions. This plot lies very close to the ideal line, though

as a result of using an exponential distribution to generate trip distances, the simulated distribution has a lighter tail than the observed distribution. This is reflected also in the histogram, wherein the simulated distance distribution (purple) lies above the observed distribution (blue) and does not stretch as far to the right.

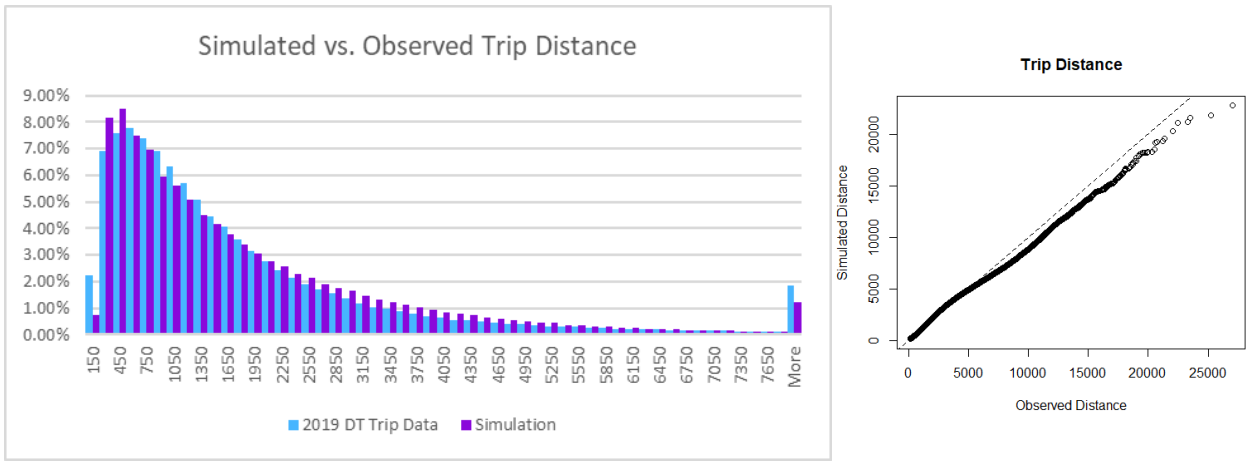

Figure 4.7: Combined histograms and QQ plot comparing observed vs. simulated trip distances

4.5.2 Route

Once the trip distance was determined, a trip route was created using the location of a chosen scooter and the relative weights of surrounding edges. Neither the aggregate data nor the trip data set included route information at a particularly fine granularity, making it difficult to directly compare simulated route information to real world traffic. Although the trip data collected in 2019 included origin and destination coordinates for each trip, there was no discernable geographical trend in trip behaviour that could direct simulated route generation. Thus, the origin point for each new trip was determined by randomly selecting an available scooter with a non-empty charge and using the scooter's current location. The route for each trip was then determined by iteratively adding neighbouring edges, selected at random using the reported daily trip volumes from 2020 to weight the probability of selecting any given edge, until the target trip distance was reached.

To approximate the forward momentum of a hypothetical rider, and to reduce the risk of a scooter trip simply travelling back and forth along the same set of high-volume edges, the route selection method prevents directly backtracking across the current edge unless the edge leads to a dead end. While this method does not prevent cyclical trip routing, it does reduce the number of repeated edges. Moreover, wide variation were observed in the 2019 trip data between the reported trip distance and distance between starting and ending coordinates, suggesting that cyclical trips are not uncommon in normal rider behaviour.

4.5.3 Speed

Finally, a trip speed is randomly selected from an empirical distribution with a lower bound determined by the trip distance. Because the distribution of trip speeds observed in 2019 did not clearly match any established statistical distribution and because the trip speeds were constrained by a fixed and finite range with only limited variation by time of day, the trip speeds were modelled using the empirical distribution directly, after filtering out any reported average trip speeds of greater than 30 kph (8.33 mps). This distribution was used to select a 1 kph interval for trip speed, and then the actual trip speed was selected from that interval using a uniformly distributed random variable.

In addition to the probability distribution constructed from observed data, the generated trip speeds are determined with consideration for the lower bound identified in Chapter 3, which showed a strict correlation between trip distance and minimum average speed. Thus, the simulation first generates the trip distance, then uses this value to set a lower bound on the speed distribution, before finally selecting a trip speed from the remaining range of values according to the empirical distribution.

The histogram given in Figure 4.8 shows a relatively close match between the simulated and observed speed distributions, though the simulated distribution (shown in purple) has a distinct step-wise variation, reflecting the uniform selection of precise speeds over each 1 kph interval. The QQ plot, likewise, gives a near perfect match between the two distributions.

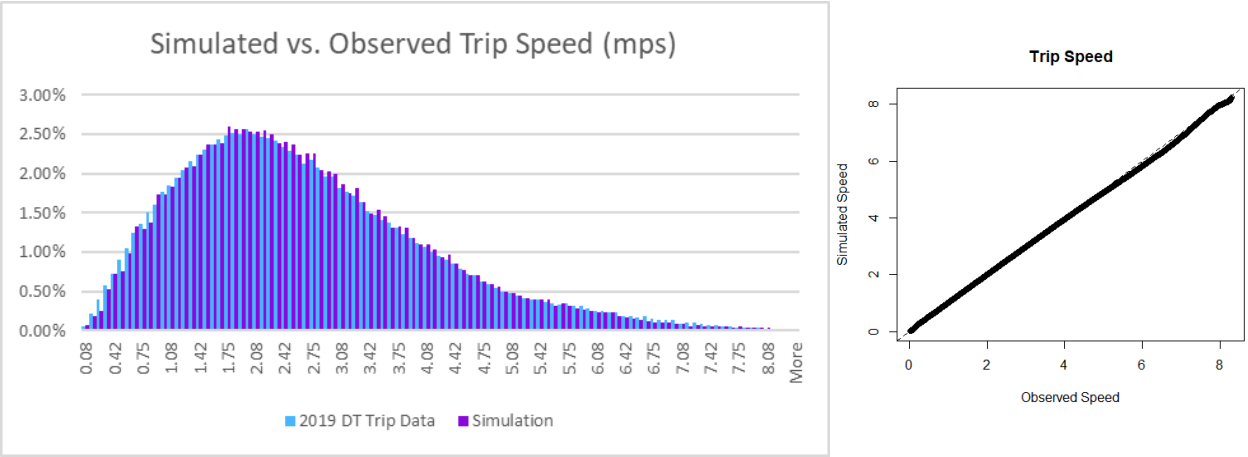

Figure 4.8: Combined histograms and QQ plot comparing observed vs. simulated trip speeds

4.5.4 Duration

In order to maintain a reasonable correlation between trip distance and trip duration, while still respecting the speed limitations of the e-scooter specifications, only the trip distance and trip speed were randomly generated for each trip, with the duration being determined as a function of these values. Thus, the simulated trip durations are difficult to validate against the observed durations because they are not being modelled directly, and the difference between the simulated and observed durations can be seen clearly in Figure 4.9. In particular, the distribution of simulated trip durations has an earlier and lower peak and a longer tail, indicating a higher number of very short-duration trips, and a much higher number of very long-duration trips.

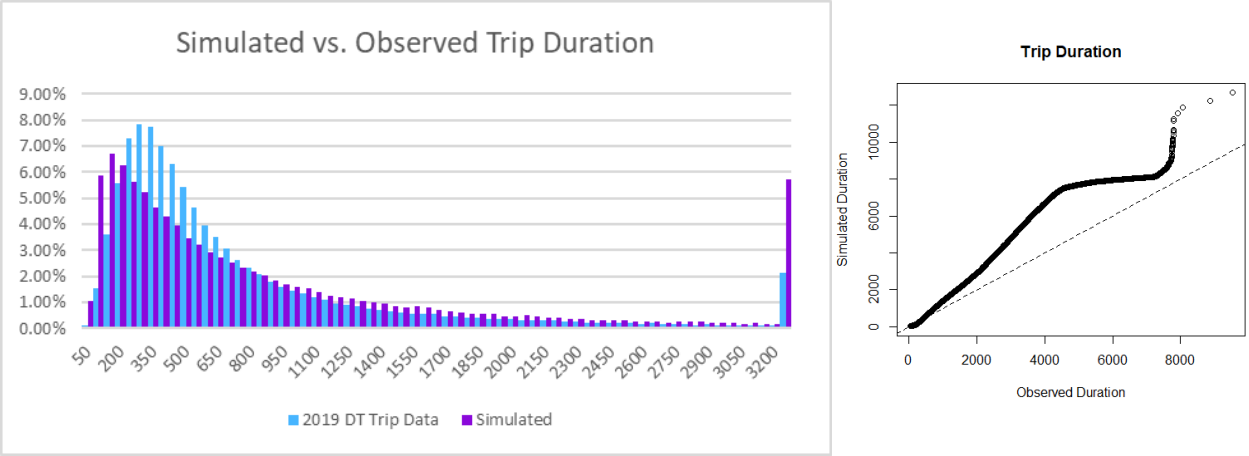

Figure 4.9: Combined histograms and QQ plot comparing observed vs. simulated trip durations

Although the simulated duration is less closely matched to the empirical trip characteristics than either trip distance or trip speed, this metric has no direct impact on battery usage and is only likely to affect the number of e-scooters in use at one time. Moreover, this method of randomly generating speed and distance from specified distributions and determining duration from these values allows for the most fluid correlation of distance and duration and accounts for the observed correlation between distance and speed.

4.6 Summary

This chapter has discussed the development of a discrete-event simulation model in Java. The model uses geographic e-scooter data from 2020 to create a representative simulation map of downtown Calgary. E-scooter objects are modelled using a mathematical battery model and placed on edges around the map. New trips are generated according to a Poisson arrival process, with the trip distance and speed being selected at random from their respective distributions. This workload model produces trip volumes, distances, and speeds that are comparable to the empirical data. This model provides the basis for the simulation experiments described in Chapter 5.

5 Simulation Results

This chapter describes the simulation experiments conducted and offers analyses of the results[16]. Section 5.1 discusses the impacts of varying the fleet size in the simulation and recommends an ideal range for the number of scooters operating in the downtown. Section 5.2 discusses placement strategies for additional SNG parking zones and recommends ideal strategies for increasing utilization and decreasing collection costs. Section 5.3 discusses the placement and number of e-scooter battery charging stations and gives specific and general recommendations on their placement. Section 5.4 summarizes the findings of this chapter.

5.1 Fleet Size

In 2019, there were 1500 scooters deployed throughout the city, and although that number rose as high as 2,300 (out of a maximum limit of 2,800) in 2020, the City later opted to cap the number of e-scooters at 1500 [47]. The aggregate data collected in 2020 showed approximately 40% of parking events took place within the six primary communities that make up the downtown, suggesting a fleet size of around 600 scooters within the downtown. One of the first experiments conducted using the simulation model was to run the simulation using various fleet sizes ranging from 100 to 1600 scooters and examine the impacts of the changes in fleet size on relevant performance metrics such as the number of successful or unserved trips per day, the time and driving distance required to collect scooters to be recharged, and the approximate utilization of the e-scooter fleet. The results from these experiments are given in Table 5.1.

[16] A subset of the results presented in this chapter have been accepted for publication and presentation at the IEEE MASCOTS 2021 conference [33].

Table 5.1: Impacts of e-scooter fleet size on fleet usage and e-scooter collection in downtown Calgary

Number of Scooters	100	200	400	800	1600
Max scooters in use	100	182	208	199	195
Avg. scooters in use	42.3	59.6	66	65.3	64.8
Successful trips per day	3656	5227	5753	5750	5732
Unserved trips per day	2086	557	0	0	0
% Trips ended at SNG	2.87%	2.99%	2.97%	2.95%	2.90%
Avg. collection time	1:24:41.3	1:48:34.9	2:01:03.8	2:01:47.6	1:55:21.1
Avg collection distance	24.523 km	28.462 km	30.662 km	29.684 km	27.944 km

The outputs from these experiments reveal several interesting trends. The first is that although the maximum and average number of scooters in use at one time rises when the fleet size in the downtown area is increased from 100 to 200, or 200 to 400, these values appear to reach a plateau and do not continue to rise with further increases in the number of available scooters in the study area. This is likely an example of Little's law, a well-known principle in queuing theory for estimating the number of customers in a system at one time [25]. Using the average intertrip time of our simulation, as well as the average trip duration, the expected average number of scooters in use at one time is given in Equation 11:

$$numScootersInUse = \frac{averageTripDuration}{averageInterTripTime} = \frac{984.41s}{15.01s} = 65.59. \quad (11)$$

When the number of unserved trips falls to approximately zero and all demand is being met, the simulation averages approximately 65 scooters in use at one time. The difference between the estimate given in Equation 10 and the measured value is likely a result of variations in ITTs and trip distances throughout the day.

Table 5.1 also shows that, using an approximation of 2020 traffic volumes, almost all rider demand within the simulation is met with a fleet size as small as 400. This suggests that the appropriate number of scooters to satisfy demand in the downtown lies nearer to 400 than 800

scooters, though additional runs of the simulation indicate that if ridership continues to increase the necessary fleet size increases correspondingly.

Finally, the time and distance required to collect depleted scooters increases slightly as the number of scooters increases. The percentage of trips ending in a SNG parking zone initially increases, but decreases again as the e-scooter fleet grows larger. These trends indicate that finding the appropriate number of scooters is a careful balance between limiting the costs of collection (operator costs) and the number of improperly parked scooters cluttering pedestrian pathways (non-user costs) and ensuring that sufficient rider demand is met (user costs). For the remaining experiments, a default fleet size of 500 scooters was used.

5.2 Parking

One of the key challenges identified by the City of Calgary's mid-pilot report was an excess of improperly parked scooters. To address this problem, several SNG zones, consisting of small, dedicated parking areas that could each accommodate approximately six scooters, were installed in the downtown area to facilitate proper e-scooter parking. The 2020 aggregate data included GEOJSON files specifying the location of 23 SNG zones, which are used as the baseline for the simulation model. Their placement is given in Figure 5.1 below.

Figure 5.1: SNG scooter parking zones identified in 2020 location data

The second set of simulation experiments involved varying the number, size, and placement of SNG zones within the downtown area. We examined the impacts of these changes on the number of trips ended at an SNG zone and the time and distance required to collect the scooters. Four different strategies were considered for the placement of additional SNG zones which would increase the total number of available parking spaces by factors of two, four, six, eight, and ten. The simulation model assumes each SNG zone can accommodate exactly six scooters and does not account for viable parking areas in the ‘furniture zones’ of the sidewalk which are widely variable and difficult to model accurately.

5.2.1 Increased Size of Parking Zones

The first and simplest strategy was to expand the areas identified in the aggregate data to accommodate more scooters. In a real-world implementation, this expansion would be necessarily limited by the available space and the need for non-scooter infrastructure, and not every existing SNG zone could realistically be expanded to accommodate sixty e-scooters, but for the purpose of comparison with the other strategies, the same scalar modifiers were used.

The results of this set of experiments are given in Table 5.2 and show that simply increasing the size of the SNG zones has very little impact on any of the relevant performance metrics. In fact, the percentage of trips ending at an SNG zone actually decreases, though not by any significant margin. It is not terribly surprising that increasing the size of the SNG zones is an ineffective method of increasing utilization, as these simulation experiments measured only trips that ended organically at an SNG zone and did not account for the possibility of riders modifying their trip depending on proximity to available parking, but it does suggest that the baseline parking strategy does occasionally see SNG zones at maximum capacity.

Table 5.2: Impacts of increasing parking space at existing SNG zones

Parking Scaling Factor	Baseline	2x	4x	6x	8x	10x
% Trips ended at SNG	3.00%	3.00%	2.92%	2.99%	2.99%	2.99%
Avg. Collection Time	2:01:41.4	2:01:59.6	2:02:10.6	2:02:45.6	2:02:45.6	2:02:45.6
Avg Collection Distance	30.19 km	30.64 km	30.46 km	30.58 km	30.58 km	30.58 km

5.2.2 Additional Parking Zones Placed at Random

The second strategy considered was to place additional SNG locations at random throughout the downtown area. The same randomized placement was used for each of the five scaling factors, meaning that the SNG locations used at each scaling factor included all the locations used at smaller scaling factors. The locations selected are shown in Figure 5.2.

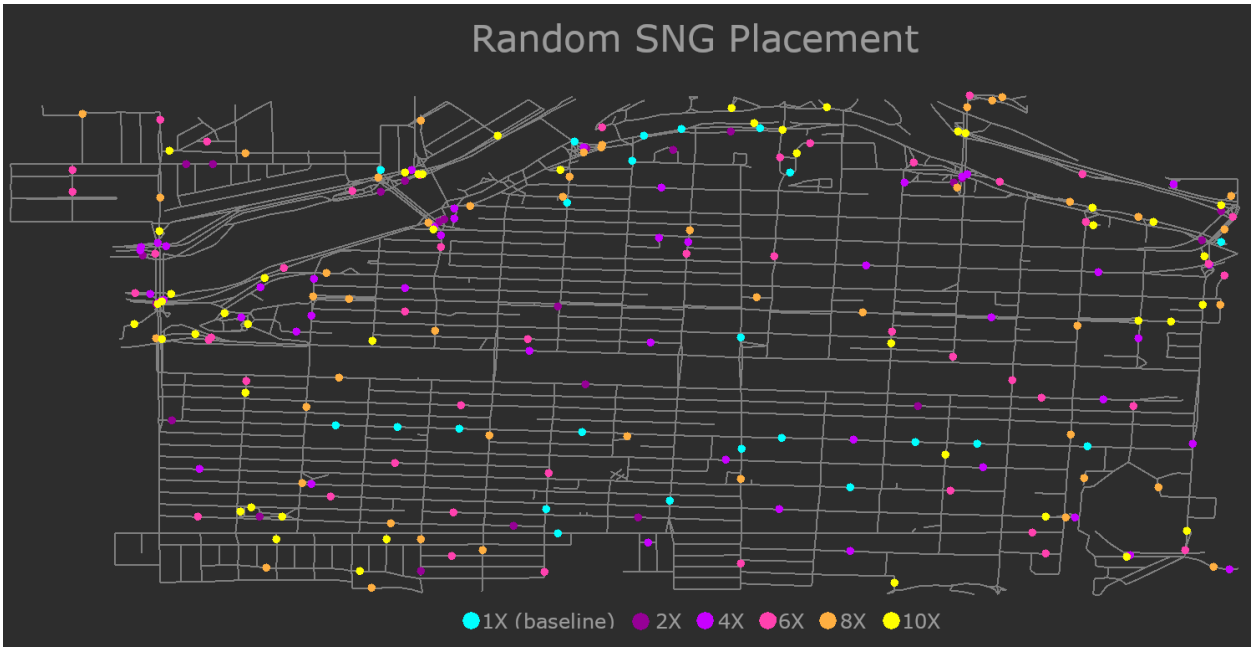

Figure 5.2: Additional SNG randomly placed parking zone locations at various scaling factors

The results of these experiments, given in Table 5.3, show a much greater impact from increasing the number of available parking spaces than was seen in the first round of SNG placement experiments, with the percentage of trips ending with a successfully parked scooter more than tripling at 10x scale.

Table 5.3: Impacts of installing additional SNG parking zones at random locations

Parking Scaling Factor	Baseline	2x	4x	6x	8x	10x
% Trips ended at SNG	3.00%	3.98%	5.72%	7.64%	9.20%	10.55%
Avg. Collection Time	2:01:41.4	2:03:01.8	2:01:11.1	2:01:08.0	2:01:41.7	2:01:45.1
Avg Collection Distance	30.19 km	30.93 km	29.92 km	29.93 km	30.29 km	30.21 km

5.2.3 Additional Parking Zones Placed by Edge Length

The third strategy was to systematically assign additional SNG zones on the longest edges, which translated practically to placing additional SNG zones only on avenues (east-west streets). The placement of these SNG zones is given in Figure 5.3.

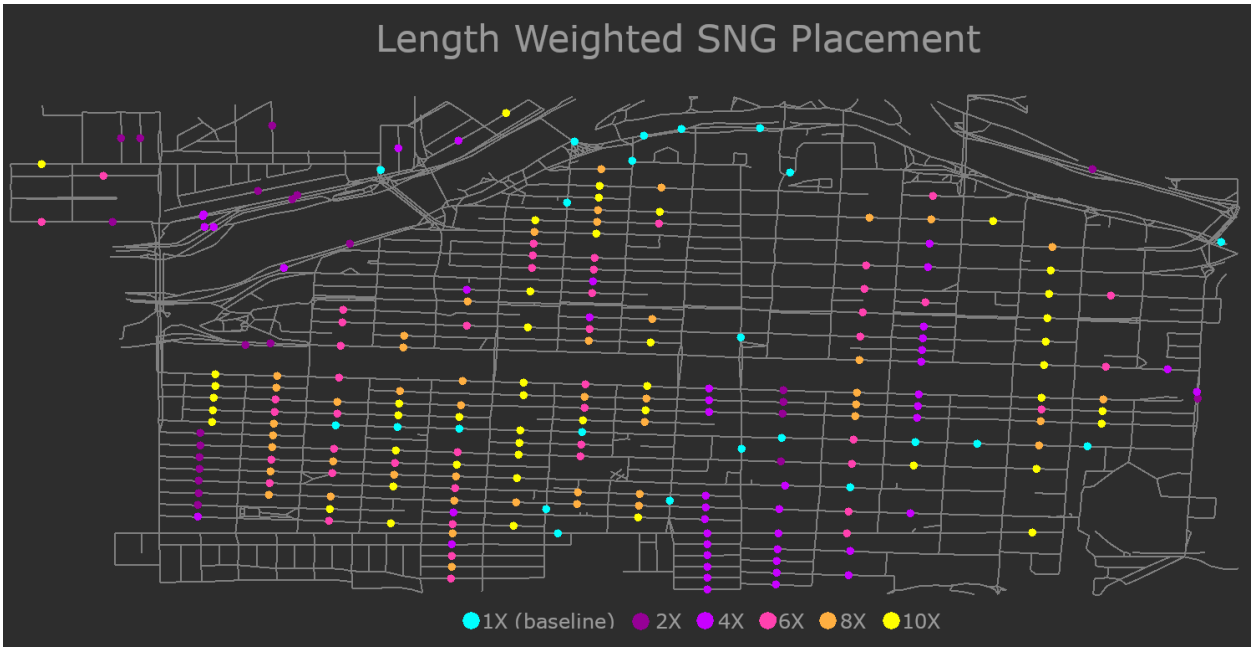

Figure 5.3: Additional SNG parking zone locations by edge length at various scaling factors

The results of these experiments are given in Table 5.4. This strategy proved more effective than either of the first two strategies, with the portion of trips successfully parked at an SNG zone reaching as almost as high as 20%. The effectiveness of this strategy may be slightly biased by the simplifying assumptions of the simulation model, namely the route generation method that appears slightly more likely to reach the target trip distance along longer edges, and the lack of consideration for trips being modified to find parking. This strategy produces a much higher percentage of SNG parking events than was seen using the previous strategy.

Table 5.4: Impacts of installing additional SNG parking zones according to edge length

Parking Scaling Factor	Baseline	2x	4x	6x	8x	10x
% Trips ended at SNG	3.00%	4.30%	8.25%	12.22%	16.08%	19.72%
Avg. Collection Time	2:01:41.4	2:01:40.3	2:01:49.5	2:02:01.0	2:02:20.1	2:00:56.8
Avg Collection Distance	30.19 km	30.02 km	30.26 km	30.25 km	30.47 km	29.90 km

5.2.4 Additional Parking Zones Placed by E-Scooter Traffic Volume

The last and most effective strategy considered was to place additional parking areas according to the e-scooter traffic volumes across each edge, resulting in dense concentrations of

SNG zones along the River Walk and along the southern portions of 4th Street and 5th Street, as shown in Figure 5.4.

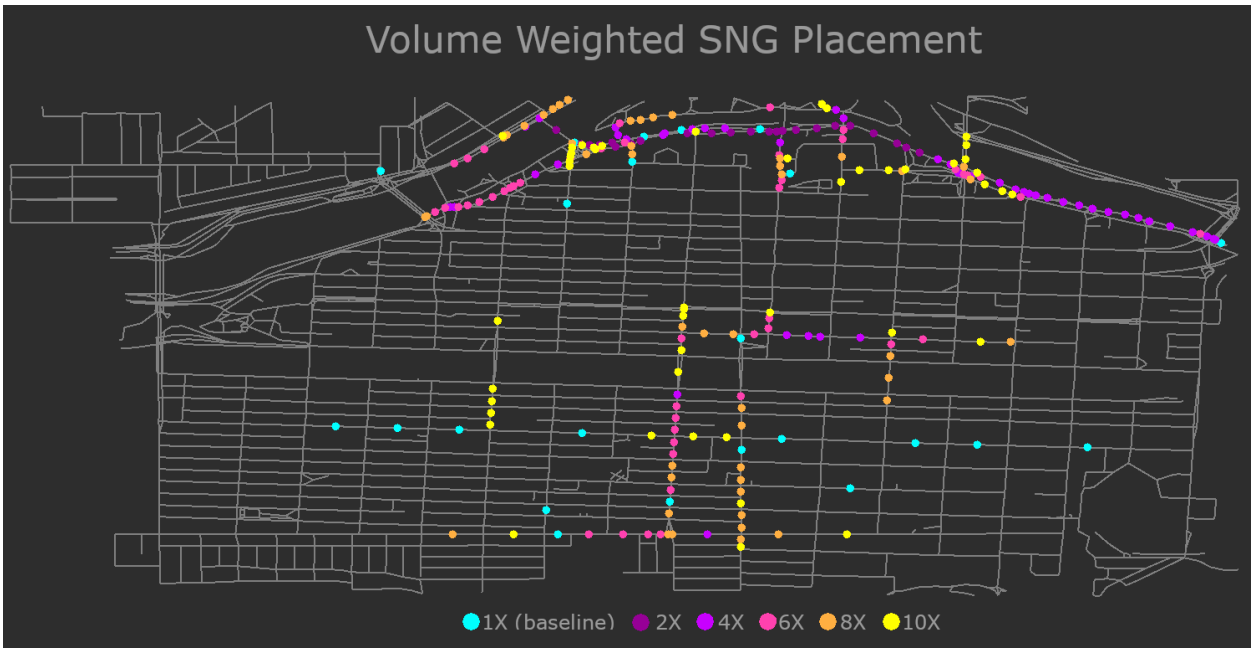

Figure 5.4: Additional SNG parking zone locations by traffic volume at various scaling factors

This placement strategy saw marked increases in trips parked at an SNG zone across all scaling factors, though with diminishing returns. This strategy also outperformed each of the other three strategies across all scaling factors, with the percentage of trips parked at an SNG zone reaching as high as 22%. The results of this round of experiments are given in Table 5.5.

Table 5.5: Impacts of installing additional SNG parking zones according to edge traffic volume

Parking Scaling Factor	Baseline	2x	4x	6x	8x	10x
% Trips ended at SNG	3.00%	5.95%	10.35%	14.41%	18.95%	22.25%
Avg. Collection Time	2:01:41.4	2:02:14.2	2:01:40.6	2:01:07.2	2:02:16.9	2:01:53.6
Avg Collection Distance	30.19 km	30.46 km	30.09 km	29.84 km	30.24 km	30.24 km

5.2.5 Impacts of Extended Trips

Finally, each of the four rounds of experiments was repeated with a modification to the simulation allowing for some percentage of the trips ending on an edge with no available parking

to be diverted to an adjacent edge with a free parking space in an SNG zone. This process was carried out twice, first with a 25% and then with a 50% chance of modifying a trip.

Figure 5.5 shows a comparison between the percentage of trips successfully parked at an SNG zone using the four different SNG placement strategies with 0%, 25%, and 50% chance of modifying a trip to find parking. This graph reveals three particularly interesting trends.

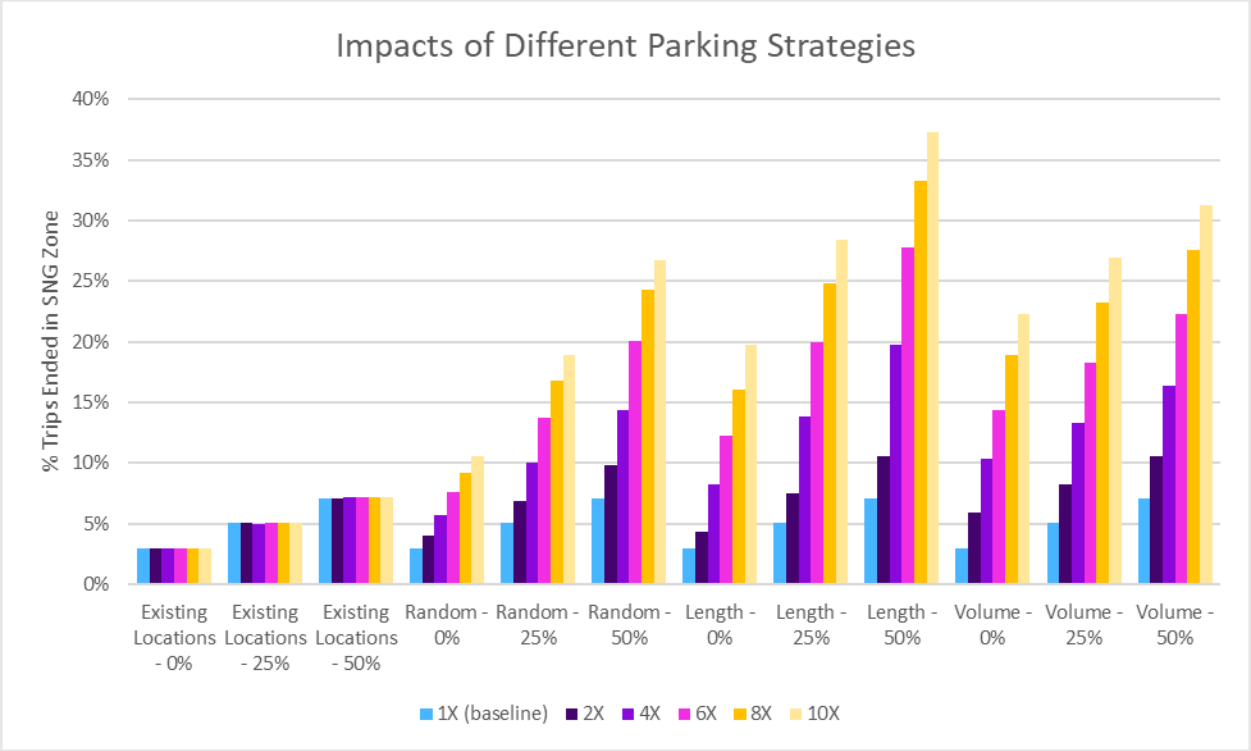

Figure 5.5: Impacts of four different parking strategies with 0%, 25%, and 50% chance to extend scooter trip to adjacent block to find parking

The first trend is that modifying the simulation to allow some percentage of trips to be extended or truncated as needed to find parking on an immediately adjacent edge resulted in marked improvement across all SNG placement strategies. This is a predictable outcome, as this modification to the simulation effectively increases the range of each SNG parking zone by as many as six edges. It also suggests that the increase in trips successfully parked at an SNG zone could be further magnified by increasing the number of adjacent edges by which to extend or truncate an e-scooter trip. However, achieving this behaviour amongst the real-world population

of e-scooter users would likely require the implementation of incentives for parking scooters in an SNG zone, such as offering a discount on that trip or future trips.

The second notable trend is that increasing the size of existing SNG zones continued to have minimal impact on the effective utilization of parking zones even when the percentage of trips that could be extended to find parking was increased, although the baseline utilization was higher. By contrast, the random and length-weighted placement strategies both saw distinctly greater utilization increases between scaling factors when the chance of extended trips was increased, in addition to the rise in baseline utilization.

The third trend is that although the SNG placement strategy that favoured *high-traffic* edges clearly yielded the highest SNG utilization in the first round of experiments, the SNG placement strategy that favoured *long* edges was the most effective strategy when trips were permitted to be extended or modified. This is likely because the length-weighted placement strategy resulted in the most evenly and broadly distributed SNG locations, maximizing the number of edges with an SNG zone or adjacent to an SNG zone. By comparison, the volume-weighted placement strategy created dense clusters of edges with parking, meaning that most edges adjacent to an edge with parking already contained an SNG zone, effectively minimizing the impact of extended trips.

5.3 Battery Charging Stations

The final round of experiments assessed the impact of installing one or more public e-scooter battery charging stations in the downtown on the number of unserved trips, and the time and distance required to collect e-scooters to be recharged. Each of the twenty-three SNG locations identified in the previous section were considered as possible battery charging station locations

(blue, *A*-*W*), as well as ten additional locations selected by highest traffic volume (green, *a*-*j*), as shown in Figure 5.6.

Figure 5.6: Possible locations for a 6-bay e-scooter battery charging station

5.3.1 Sensitivity Study

In order to determine the value of relevant metrics, like the percentage of trips ended at an available charging bay and the average collection time, as measures of performance for optimizing placement, a sensitivity study was conducted comparing these metrics from multiple experiments while varying one parameter at a time, including using different seeds for random number generation (57391 vs. 15397), increasing and decreasing e-scooter battery capacity by 25% (1687.5 kJ vs. 1012.5 kJ), increasing and decreasing fleet sizes by 25% (625 scooters vs. 375 scooters), and increasing and decreasing low-battery thresholds for scooters to be collected and recharged by 25% (31.25% threshold vs. 18.75% threshold).

The results of this sensitivity study are given in Figure 5.7 and Figure 5.8. The comparison of the percentage of trips ending at an available charging bay shows a largely consistent behaviour across all scenarios with minimal variation. The largest variations are at battery charging locations *a*, *U*, *V*, and *B* and result primarily from reductions in the number of scooters or the low-battery

charging threshold for collecting and recharging scooters. Although the comparison of collection times shows much more distinct variation between various simulation conditions, the general *shape* of each graph is both largely similar between different conditions and largely flat, aside from a few small but distinct reductions at locations *R*, *V*, *a*, and *c* which mirror peaks in Figure 5.7.

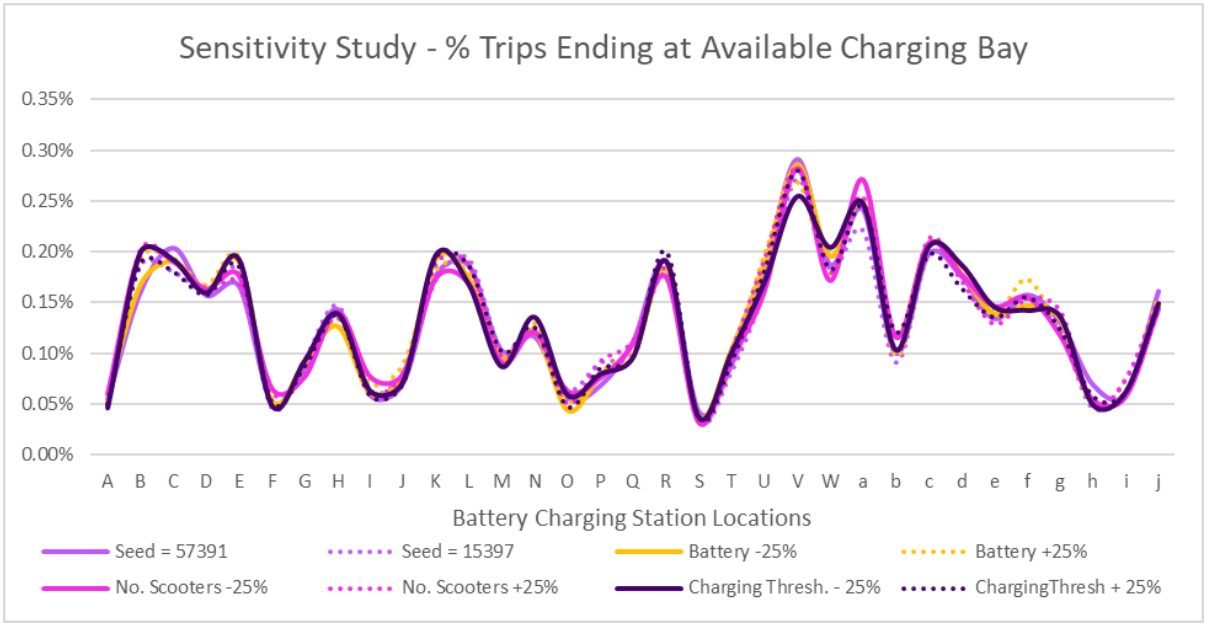

Figure 5.7: Sensitivity study comparing percentage of trips ending at an available charging bay under varied simulation conditions

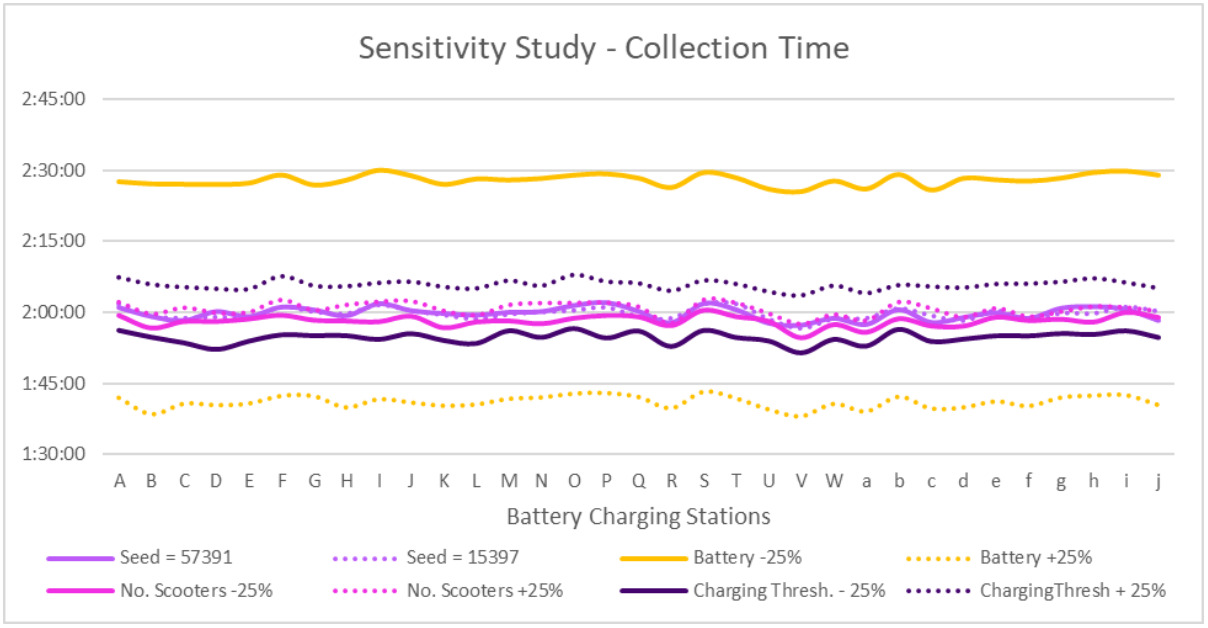

Figure 5.8: Sensitivity study comparing time required to collect scooters with low charge under varied simulation conditions

5.3.2 Placement of Battery Charging Stations

Finally, two additional rounds of experiments were conducted, allowing for the placement of first two, and then three battery charging stations on the simulation map. After running the initial sensitivity test, the ten candidate locations with the highest average percentage of trips ending at an available charging bay were selected as candidate locations for the second round of experiments. These locations are given in Table 5.6. Figure 5.9 shows a comparison of the percent of trips ended at an available charging bay and the average collection time for each pair of candidate locations.

Table 5.6: Single candidate locations for placement of charging stations

Location	% Trips Ending at Charging Bay	Average Collection Time
L	0.1801%	2:00:20
E	0.1818%	2:00:24
R	0.1843%	1:59:22
K	0.1848%	2:00:23
W	0.1854%	2:00:20
B	0.1873%	2:00:08
C	0.1903%	2:00:21
c	0.2039%	2:00:00
a	0.2477%	1:59:02
V	0.2770%	1:58:06

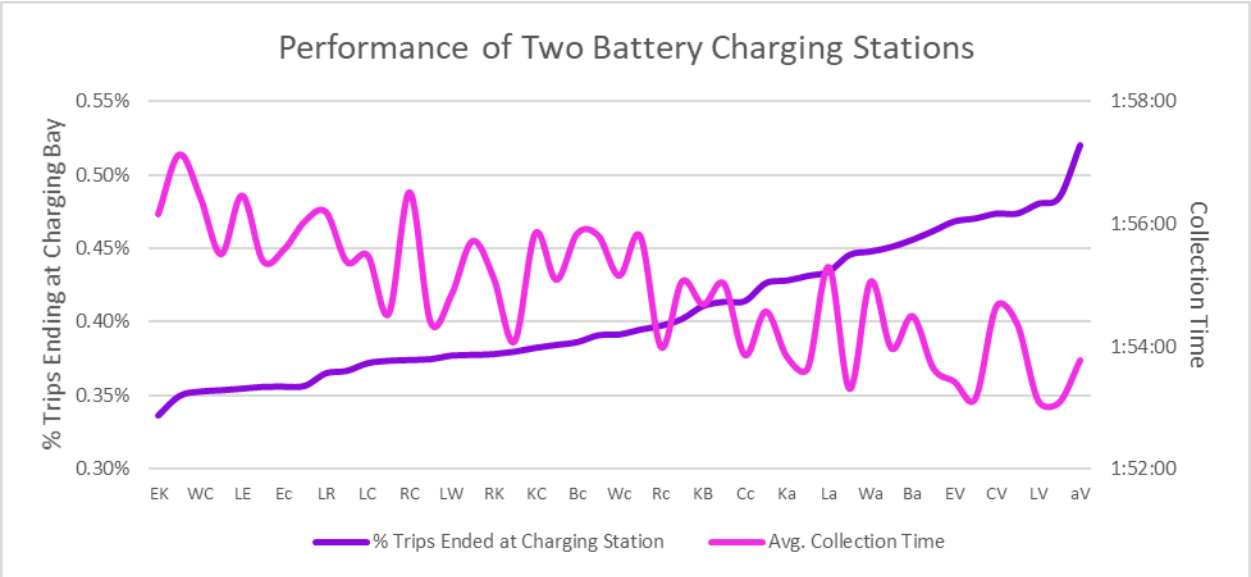

Figure 5.9: Relative performance of different pairs of battery charging station locations

After running the second round of experiments, the process was repeated, identifying the top performing locations to be used as candidate locations for the third round of experiments, those being locations *R, W, B, C, c, a,* and *V*. Figure 5.10 gives a comparison of each combination of three candidate locations. A comparison of the top ten best performing scenarios from each round of experiments is given in Figure 5.11.

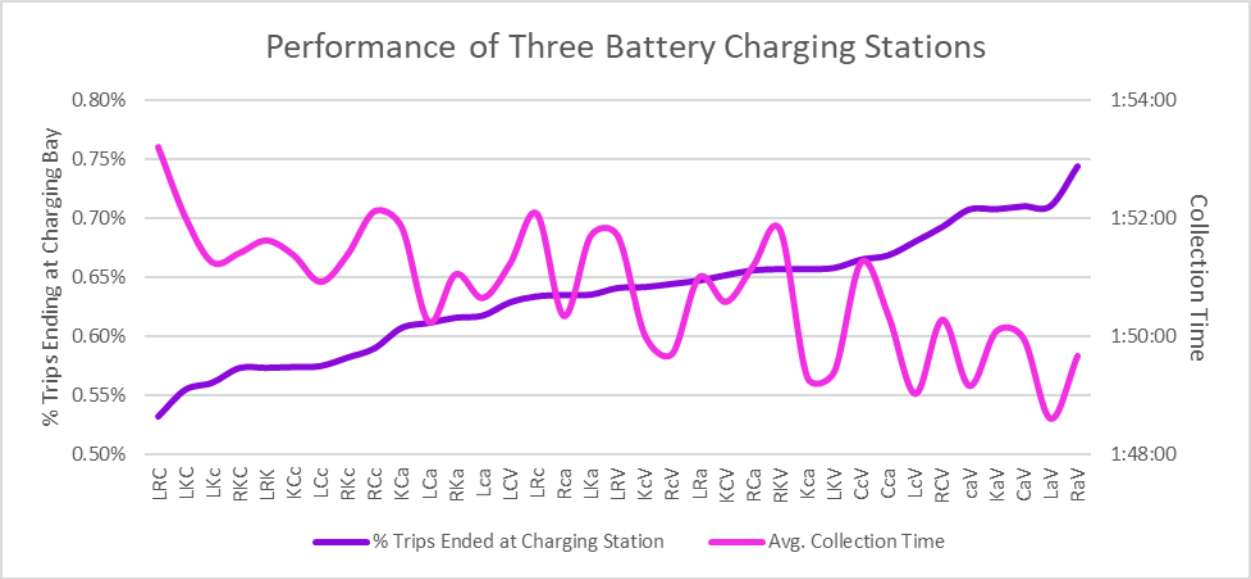

Figure 5.10: Relative performance of different trios of battery charging station locations

The results of these experiments show two particular trends. The first is that, as one would expect, the number of trips ending at a battery charging station with an available bay increases as the number of battery charging stations increases. Interestingly, however, the increase from one charging station to two is more significant than either the increase from no battery charging stations to one charging station or the increase from two charging stations to three.

The second trend is that the average time required to collect scooters for recharging tends to decrease as the number of trips ending at an available charging bay increases, with the most efficient charging station placement scenario dropping the average collection time from its baseline value of two hours and one minute to just over one hour and forty-nine minutes, a

reduction of approximately 10.5%. However, the relationship between the increase in charging station utilization and the decrease in collection time is not strict. The best performing placement scenario in terms of battery charging station utilization (*RaV*) is only the sixth-best performing scenario in terms of the reduction in collection time. Conversely, the best performing placement scenario in terms of reduced collection times (*LaV*) is second in terms of battery charging station utilization. Moreover, the variation between collection times for different battery charging station locations becomes more pronounced as more stations are added to the system.

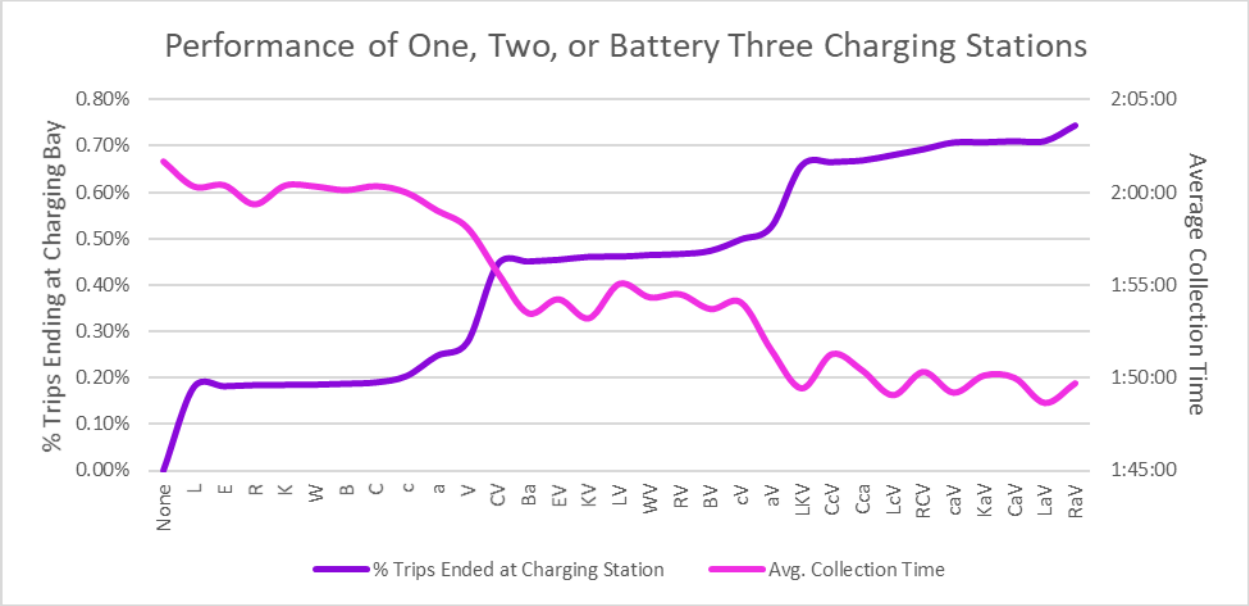

Figure 5.11: Percent of trips parked at a charging station and e-scooter collection time for top performing locations of 1, 2, or 3 charging stations

What's curious from the results from this area of experimentation is a lack of consistency between the characteristics of the high-performance candidate locations. Generally, locations along 17th Avenue and along the River Walk tend to perform better than locations along north-south streets or that lay towards the edges of the simulation area. However, of the nine candidate locations that lie along or adjacent to 17th Avenue, only four were selected to be used in the second round of experiments (*V, C, B,* and *R*) while one location (*M*) was not even in the top half of locations when ranked by battery charging station utilization. All ten of the additional locations

selected by edge volume lie along the River Walk, including location *a*, which was one of the best performing locations across all three rounds of experiments. However only two (*a* and *c*) were identified as candidates for the second and third rounds of experiments, and three of the additional candidate locations were among the worst performing half of locations.

The only consistency between the 'top' locations that distinguished them from the remaining candidate locations were increased edge length and e-scooter traffic volume. The average edge length of the best-performing locations was 60% greater than the average of all candidate locations and 138% larger than the average of all edges in the map. The average e-scooter traffic volume across edges with the best-performing locations was 3% greater than the average of all candidate locations and 366% larger than the average of all edges in the map.

5.4 Summary

This chapter has discussed the experiments conducted using the simulation model.

Varying the simulated fleet size demonstrated the careful balance between meeting user demand and managing operator costs and improperly parked scooters. These experiments suggested that the optimal range for e-scooter fleet size in the downtown is 500-600 scooters.

Increasing the number of SNG parking zones using various placement strategies showed that simply increasing the size of the zones was ineffective at increasing SNG zone utilization. Adding parking on longer, east-west streets more effectively increased SNG zone utilization, particularly when trips were permitted to be extended or modified to find parking, but also increased the time and distance required to collect scooters. Adding parking along streets with high volumes of e-scooter traffic proved effective at increasing SNG utilization even without permitting trips to be modified, and created minimal increase in collection costs.

Adding one, two, or three charging stations slightly reduced average collection time, even with as little as 0.2% of trips ending at a battery charging station with an available charging bay. The locations that resulted in the highest levels of utilization tended to be longer, higher volume streets along 17th Avenue and the River Walk.

6 Conclusion

E-scooters, and shared micromobility more generally, are rapidly gaining a strong foothold within the domain of urban transportation. They have the potential to offer many benefits to an urban population, such as reducing the reliance on privately owned and/or internal combustion engine vehicles, facilitating the use of public transit, and combatting transportation inequity. Yet in order to effectively fulfill the promise of shared-micromobility, policymakers and e-scooter operators will have to grapple with balancing rising demand for shared micromobility options with the costs and infrastructure demands of storing and maintaining these vehicles.

This thesis has helped to address these social and technical issues by studying e-scooter usage patterns in the City of Calgary and developing a simulation model to study different management strategies for shared micromobility. This chapter summarizes the research and observations outlined in this thesis and discusses conclusions and future work.

6.1 Thesis Summary

This thesis has discussed the growing popularity of SMMSs and their role within the transportation landscape, and examined the impact of different fleet management policies on specific performance metrics. The thesis was structured as follows:

- Chapter 1 introduced the focus of this thesis, and outlined the primary motivations, objectives, and contributions of the research.
- Chapter 2 provided a historical and cultural context for the development and use of SMMSs and shared e-scooters in particular. The chapter also discussed the bodies of work relating to shared mobility research, workload characterization from empirical data, and systems modelling and simulation.

- Chapter 3 described the available datasets on e-scooter activity in Calgary and their limitations. The data analysis process was described and specific trends and statistical distributions that characterized the e-scooter data were identified.
- Chapter 4 described the construction of a custom-built, dedicated simulation environment in Java. The chapter discussed the development of a simulation model from the workload characterization conducted in Chapter 3 and validated the simulation model against the empirical data.
- Chapter 5 outlined the structure of three sets of experiments relating to (1) fleet size, (2) SNG parking zone placement, and (3) placement and number of e-scooter battery charging stations. The chapter presented the results of each of the experiments, describing the principal impacts on performance metrics and identifying policy guidelines.

6.2 Thesis Contributions

There are three main technical contributions in this thesis, namely a workload characterization study, the development of a simulation model, and simulation experiments to evaluate management strategies for Calgary's e-scooter system. These contributions are briefly summarized next.

This thesis has presented a detailed workload characterization of shared e-scooter usage in downtown Calgary, using empirical data from 2019 and 2020. The results from this analysis include the temporal variations in traffic volumes and statistical distributions of trip characteristics.

A simulation model was developed from these analyses and used in the creation of a discrete-event simulation environment for testing different changes to the e-scooter program and examining their impact on performance metrics relevant to the City and the e-scooter operators, as

well as the populations of e-scooter users and non-users. These included the ability of the e-scooter fleet to meet the transportation demands of e-scooter users, the frequency with which scooters were properly parked in a dedicated parking area, and the costs to the operator of collecting scooters for recharging.

Finally, experiments were conducted using the constructed simulation model to measure the impact of different fleet management policies on these performance metrics. These experiments revealed specific trends in fleet performance and offered insights that could help to inform future policy decisions.

6.3 Conclusions

6.3.1 Workload Characterization

Analysis of the empirical e-scooter data from 2019 and 2020 revealed several observations about how, when, and where the e-scooters were used:

- *Geographic Variation:* In both 2019 and 2020, approximately 67% of e-scooter trips in Calgary took place within the downtown. Route data from the downtown area showed that the busiest downtown avenues were the River Walk, 8th Avenue, 12th Avenue, and 17th Avenue, and the busiest downtown streets were 4th Street and 5th Street.
- *Temporal Variation:* In 2019, hourly e-scooter traffic volumes displayed consistent diurnal variation and a distinct tri-peaked structure on weekdays, with increased volumes during morning and evening rush hour, as well as at lunch hour. This shape was most clearly defined when data was isolated to the downtown but still visible in general traffic volumes. In 2020, the traffic patterns were different with much less

pronounced peaks. This difference likely reflects the changes in transportation requirements as a result of COVID-19 public health mandates.

- *Trip Distance:* The majority of e-scooter trips are less than 2 kilometres, with the average trip distance being 1.74 kilometres in 2019 in the downtown and approximately 1.5 kilometres in 2020, with the average hourly trip distance showing distinct diurnal variation. The distribution of trip distances in the downtown appears to closely match an exponential distribution in the main body of the distribution but deviates toward the tail.
- *Trip Duration:* Most e-scooter trips are less than 15 minutes, with the average trip duration in 2019 in the downtown being approximately 12.5 minutes. The observed trip durations also showed a fairly strict upper bound at just over two hours.

6.3.2 Simulation Outcomes

The three sets of experiments described in Chapter 5 each offered specific insights to inform governmental policy regarding e-scooters or fleet management strategies for e-scooter operators.

- *Fleet Size:* At demand levels consistent with the trip volumes observed in 2020, the number of e-scooters required to meet that demand within the downtown area lies between 400 and 800. This is consistent with the City's vehicle cap of 1500 e-scooters and the estimated proportion of e-scooters residing within the downtown.
- *Parking Zones:* Investigation into the effective placement of additional SNG parking zones emphasized the value of frequency over total volume of parking spaces, particularly when accounting for the possibility of e-scooter users modifying their trips

to end at an SNG zone. In particular, giving preference to longer streets or streets with a very high volume of e-scooter traffic yields the highest utilization of SNG zones, whereas expanding the capacity of existing zones offers effectively no benefit.

- *Charging Stations:* These experiments showed that installing one or more charging stations on longer, higher volume streets along 17th Avenue and the River Walk could reduce the time required to collect scooters to be recharged by approximately 3-10%, thus lowering the fuel and labour costs to the operators.

6.4 Future Work

There are many possible directions for expanding on this research, relating to workload characterization, simulation modelling, and incorporating other mobility and micromobility services.

Because the e-scooter program was only recently introduced to Calgary, only a limited timeframe was considered for our workload characterization, but future studies could examine a longer timeframe to identify long-term variations in behaviour, seasonal variations, or investigate the impacts of the COVID-19 pandemic more thoroughly. Additional research could also compare e-scooter usage patterns with other cities with shared micromobility programs, or use trip-level trajectory data to more precisely characterize the variations in directionality of traffic.

Future research could build on this simulation model by (1) incorporating more thorough characterizations of e-scooter usage behaviour and demand from the perspective of users (e.g., pricing sensitivity, behavioural incentives, brand loyalty, last-mile access, pedestrian interactions, crowd dynamics, congestion effects), rather than just operators, (2) developing a more precise model of e-scooter battery behaviour, or one that uses trajectory data from e-scooter operators to

model directionality of trips to more closely examine the effective placement of parking zones or battery charging stations, (3) investigating the efficacy and optimal implementation of pricing incentives to encourage the use of parking zones and battery charging stations, and (4) experimenting with alternate battery charging strategies such as public e-scooter battery-swapping stations.

Further investigation into the role of e-scooters within the larger transportation landscape is also needed, to determine how e-scooters can most effectively facilitate public transportation or reduce congestion arising from large events like concerts, sports games, and the Stampede.

Bibliography

[1] R. Abduljabbar, S. Liyanage and H. Dia, "The Role of Micro-mobility in Shaping Sustainable Cities: A Systematic Literature Review", *Transportation Research Part D: Transport and Environment*, vol. 92, no. 102734, pp. 1-19, 2021.

[2] V. Alencar, F. Rooke, M. Cocca, L. Vassio, J. Almeida and A. Vieira, "Characterizing Client Usage Patterns and Service Demand for Car-sharing Systems", *Information Systems*, vol. 98, no. 101448, pp. 1-10, 2021.

[3] P. Alvarez Lopez, M. Behrisch, L. Bieker-Walz, J. Erdmann, Y.-P. Flötteröd, R. Hilbrich, L. Lücken, J. Rummel, P. Wagner and E. Wießner, "Microscopic Traffic Simulation using SUMO", in *2018 IEEE Intelligent Transportation Systems Conference (ITSC)*, pp. 2575-2582, Maui, HI, USA, 2018.

[4] K. Anderson-Hall, B. Bordenkircher, R. O'Neil and C. Smith, "Governing Micro-Mobility: A Nationwide Assessment of Electric Scooter Regulations", in *Transportation Research Board 98th Annual Meeting*, Washington, DC, 2019.

[5] A. Andwari, A. Pesiridis, S. Rajoo, R. Martinez-Botas and V. Esfahanian, "A Review of Battery Electric Vehicle Technology and Readiness Levels", *Renewable and Sustainable Energy Reviews*, vol. 78, pp. 414-430, 2017.

[6] K. Arnold, J. Gosling and D. Holmes, *The Java Programming Language*., Addison Wesley Professional., 2005.

[7] M. Barth, J. Han and M. Todd, "Performance Evaluation of a Multi-Station Shared Vehicle System", in *Intelligent Transportation Systems Conference Proceedings*, pp. 1218-1223, Oakland, CA, USA, 2001.

[8] S. Blomberg, O. Rosenkrantz, F. Lippert and H. Christrensen, "Injury from Electric Scooters in Copenhagen: A Retrospective Cohort Study", *BMJ Open*, vol. 9, no. 12, p. e033988, 2019.

[9] A. Campbell, C. Cherry, M. Ryerson and X. Yang, "Factors Influencing the Choice of Shared Bicycles and Shared Electric Bikes in Beijing", *Transportation Research Part C: Emerging Technologies*, vol. 67, pp. 399-414, 2016.

[10] O. Caspi, M. Smart and R. Noland, "Spatial Associations of Dockless Shared E-scooter Usage", *Transportation Research Part D: Transport and Environment*, vol. 86, no. 102396, pp. 1-15, 2020.

[11] L. Chen, A. Mislove and C. Wilson, "Peeking Beneath the Hood of Uber", in Proceedings of the *2015 ACM Internet Measurement Conference*, pp. 495-508, Tokyo, Japan, 2015.

[12] Z. Christoforou, A. de Bortoli, C. Gioldasis and R. Seidowsky, "Who is Using E-scooters and How? Evidence from Paris", *Transportation Research Part D: Transport and Environment*, vol. 92, no. 102708, pp. 1-15, 2021.

[13] A. Ciociola, M. Cocca, D. Giordano, L. Vassio and M. Mellia, "E-Scooter Sharing: Leveraging Open Data for System Design", in *2020 IEEE/ACM 24th International Symposium on Distribution Simulation and Real Time Applications (DS-RT)*, pp. 1-8, Prague, Czech Republic, 2020.

[14] M. Clemente, M. Fanti, G. Iacobellis and W. Ukovich, "A Discrete-Event Simulation Approach for the Management of a Car Sharing Service", in *International Conference on Systems, Man, and Cybernetics*, pp. 403-408, Manchester, UK, 2013.

[15] H. Dia and F. Javenshour, "Autonomous Shared Mobility-On-Demand: Melbourne Pilot Simulation Study", *Transportation Research Procedia 22*, pp. 285-296, 2017.

[16] J. Fong, P. McDermott and M. Lucchi, "Micro-Mobility, E-Scooters and Implications for Higher Education", UPCEA Center for Research and Strategy, 2019.

[17] A. Fotouhi, D. Auger, K. Propp, S. Longo and M. Wild, "A Review on Electric Vehicle Battery Modelling: From Lithium-ion Toward Lithium–Sulphur", *Renewable and Sustainable Energy Reviews*, vol. 56, pp. 1008-1021, 2016.

[18] S. Gössling, "Integrating E-scooters in Urban Transportation: Problems, Policies, and the Prospect of System Change", *Transportation Research Part D: Transport and Environment*, vol. 79, no. 102230, pp. 1-12, 2020.

[19] L. Greening and A. Erera, "Locating Vehicles to Improve Utilization in Micromobility Systems with Crowdsourced Repositioning", (Unpublished), pp. 1-36, 2020.

[20] K. Heineke, B. Kloss, D. Scurtu and F. Weig, "Micromobility's 15,000-mile Checkup", *McKinsey & Company Automative & Assembly*, 2019.

[21] J. Hollingsworth, B. Copeland and J. Johnson, "Are E-scooters Polluters? The Environmental Impacts of Shared Dockless Electric Scooters", *Environmental Research Letters*, vol. 14, no. 8, pp. 1-10, 2019.

[22] A. Horni, K. Nagel and K. Axhausen, *The Multi-Agent Transport Simulation MATSim*, London: Ubiquity Press, 2016.

[23] F.-H. Huang, "Exploring the Environmental Benefits Associated with Battery Swapping System Processes", *Advances in Environmental Biology*, vol. 9, no. 26, pp. 87-92, 2015.

[24] J. Jiao and S. Bai, "Understanding the Shared E-scooter Travels in Austin, TX", *International Journal of Geo-Information*, pp. 1-12, 2020.

[25] L. Kleinrock, *Queueing Systems: Volume I - Theory*, New York: Wiley, 1975.

[26] T. Kurczveil, P. López and E. Schnieder, "Implementation of an Energy Model and a Charging Infrastructure in SUMO", in *Proceedings of 1st SUMO User Conference SUMO2013*, pp. 88-94, Berlin, Germany, 2013.

[27] W. Li, Z. Pu, Y. Li and X. Ban, "Characterization of Ridesplitting based on Observed Data: A Case Study of Chengdu, China", *Transportation Research Part C: Emerging Technologies*, vol. 100, pp. 330-353, 2019.

[28] Lime, "Year End Report 2018", Lime, 2018.

[29] S. Liyanage and H. Dia, "An Agent-Based Simulation Approach for Evaluating the Performance of On-Demand Bus Services", *Sustainability*, vol. 12, no. 4117, pp. 1-20, 2020.

[30] Q. Ma, H. Yang, Y. Ma, D. Yang, X. Hu and K. Xie, "Examining Municipal Guidelines for Users of Ahared E-Scooters in the United States", *Transportation Research Part D: Transport and Environment*, vol. 92, no. 102710, pp. 1-14, 2021.

[31] G. McKenzie, "Spatiotemporal Comparative Analysis of Scooter-share and Bike-share Usage Patterns in Washington, D.C", *Journal of Transport Geography*, vol. 78, pp. 19-28, 2019.

[32] G. McKenzie, "Urban Mobility in the Sharing Economy: A Spatiotemporal Comparison of Shared Mobility Services", *Computers, Environment and Urban Systems*, vol. 79, no. 101418, pp. 1-10, 2020.

[33] R. Mclean, C. Williamson, and L. Kattan, "Simulation Modeling of Urban E-Scooter Mobility", to appear, *Proceedings of the 29th IEEE International Symposium on the Modeling and Simulation of Computer and Telecommunication Systems (MASCOTS)*, virtual conference, Nice, France, November 2021.

[34] National Association of City Transport Officials, "Shared Micromobility in the U.S.: 2018", 2018.

[35] National Association of City Transportation Officials, "Shared Micromobility in the U.S.: 2019", 2019.

[36] A. Nikiforiadis, E. Paschalidis, N. Stamatiadis, A. Raptopoulou, A. Kostareli and S. Basbas, "Analysis of Attitudes and Engagement of Shared E-scooter Users", *Transportation Research Part D: Transport and Environment*, vol. 94, no. 102790, pp. 1-14, 2021.

[37] D. Pande and A. Taeihagh, "The Governance Conundrum of Powered Micromobility Devices: An In-Depth Case Study from Singapore", *Sustainability*, vol. 13, no. 6202, pp. 1-24, 2021.

[38] J. Pfrommer, J. Warrington, G. Schildbach and M. Morari, "Dynamic Vehicle Redistribution and Online Price Incentives in Shared Mobility Systems", *IEEE Transactions on Intelligent Transportation Systems*, vol. 15, no. 4, pp. 1567-1578, 2014.

[39] Portland Bureau of Transportation, "2018 E-Scooter Findings Report", Portland, 2018.

[40] R Core Team, *R: A Language and Environment for Statistical Computing*, Vienna, 2021.

[41] A. Rahim Taleqani, J. Hough and K. Nygard, "Public Opinion on Dockless Bike Sharing: A Machine Learning Approach", *Transportation Research Record 2019*, vol. 2673, no. 4, pp. 195-204, 2019.

[42] A. Rahim Taleqani, C. Vogiatzis and J. Hough, "Maximum Closeness Centrality *k*-Clubs: A Study of Dock-Less Bike Sharing", *Journal of Advanced Transportation 2020*, pp. 1-16, 2020.

[43] D. Reck, S. Guidon, H. Haitao and K. Axhausen, "Shared Micromobility in Zurich, Switzerland: Analysing Usage, Competition and Mode Choice", in *20th Swiss Transport Research Conference (STRC 2020)* (virtual), pp. 1-18, Ascona, Switzerland, 2020.

[44] N. Sanchez, I. Martinez, L. A. Pastor and K. Larson, "Simulation Study on the Fleet Performance of Shared Autonomous Bicycles", *arXiv preprint arXiv:2106.09694.*, 2021.

[45] M. Sebastiani, R. Lüders and K. Fonseca, "Allocation of Charging Stations in an Electric Vehicle Network Using Simulation Optimization", in *Proceedings of the 2014 Winter Simulation Conference*, pp. 1073-1083, Savannah, GA, USA , 2014.

[46] A. Sedor and N. Carswell, "Shared e-Bike and e-Scooter Mid-Pilot Report", Calgary, 2019.

[47] A. Sedor and J. Oriold, "Shared e-Bike and e-Scooter Final Pilot Report", Calgary, 2020.

[48] S. Shaheen, C. Bell, A. Cohen and B. Yalchuru, "Travel Behavior: Shared Mobility and Transportation Equity", U.S. Department of Transportation, 2017.

[49] S. Shaheen, N. Chan, A. Bansal and A. Cohen, "Definitions, Industry Developments, and Early Understanding", Berkeley California: University of California Berkeley-Transportation Sustainability Research Center, 2015.

[50] S. Shaheen and A. Cohen, "Shared Micromoblity Policy Toolkit: Docked and Dockless Bike and Scooter Sharing", UC Berkeley: Transportation Sustainability Research Center, 2019.

[51] S. Shaheen, A. Cohen and I. Zohdy, "Shared Mobility: Current Practices and Guiding Principles", U.S. Department of Transportation, 2016.

[52] S. Shaheen, D. Sperling and C. Wagner, "A Short History of Carsharing in the 90's", *The Journal of World Transport Policy & Practice*, pp. 18-40, 1999.

[53] K. Smith, M. Earleywine, E. Wood, J. Neubauer and A. Pesaran, "Comparison of Plug-In Hybrid Electric Vehicle Battery Life Across Geographies and Drive Cycles", in *2012 SAE World Congress and Exhibition*, pp. 1-11, Detroit, MI, USA, 2012.

[54] F. Sprei, "Disrupting Mobility", Energy Research & Social Science, vol. 37, pp. 238-242, 2018.

[55] N.-C. Tai, D. Wu and H.-W. Jang, "Extending the Range of Electric Scooters from Fixed-Point Battery Stations by Using a Dynamic Battery Swapping Mobile Application", in

Proceedings of IEEE International Conference on Applied System Innovation, pp. 389-392, Chiba, Japan, 2018.

[56] The City of Calgary, "Electric Scooter Share Pilot Stakeholder Report Back: What We Heard", The City of Calgary, 2020.

[57] The City of Calgary, "Shared Mobility Pilot Trips", 9 April 2020. [Online]. Available: https://data.calgary.ca/Transportation-Transit/Shared-Mobility-Pilot-Trips/jicz-mxiz

[58] The City of Calgary, "Shared e-Scooter (micromobility) program", 28 May 2021. [Online]. Available: https://www.calgary.ca/transportation/tp/cycling/cycling-strategy/shared-electric-scooter-pilot.html?redirect=/scootershare

[59] P. Tice, "Micromobility and the Built Environment", *Proceedings of the Human Factors and Ergonomics Society 2019 Annual Meeting*, pp. 929-932, 2019.

[60] L. Tolomei, "Relocation Strategies for E-scooter System Optimization", Masters' Degree Thesis, Politecnico di Torino, pp. 1-69, 2021.

[61] S. Tuncer and B. Brown, "E-scooters on the Ground: Lessons for Redesigning Urban Micro-Mobility", in *Proceedings of the 2020 ACM CHI Conference on Human Factors in Computing Systems*, pp. 1-14, Honolulu, HI, USA, April 2020.

[62] W. Yakowicz, "14 Months, 120 Cities, $2 Billion: There's Never Been a Company Like Bird. Is the World Ready?", 10 December 2018. [Online]. Available: https://www.inc.com/magazine/201902/will-yakowicz/bird-electric-scooter-travis-vanderzanden-2018-company-of-the-year.html. [Accessed 21 07 2021].

[63] S. Yan, C.-K. Lin and Z.-Q. Kuo, "Optimally Locating Electric Scooter Battery Swapping Stations and Battery Deployment", *Engineering Optimization*, vol. 53, no. 5, pp. 1-16, 2020.